Inorganic Chemistry

ARTICLE

pubs.acs.org/IC

Coordination and Reductive Chemistry of Tetraphenylborate Complexes of Trivalent Rare Earth Metallocene Cations, $[(C_5Me_5)_2Ln][(\mu\text{-}Ph)_2BPh_2]$

Matthew R. MacDonald, Joseph W. Ziller, and William J. Evans*

Department of Chemistry, University of California, Irvine, California 92697-2025, United States

Supporting Information

ABSTRACT:

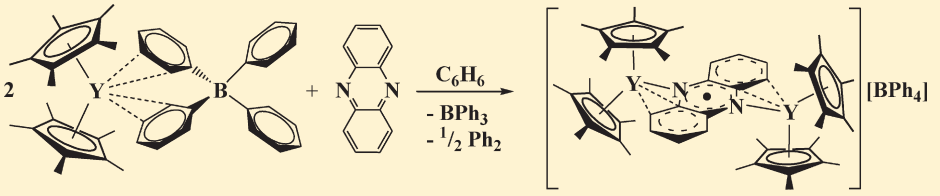

The reactivity of the tetraphenylborate salts of the rare earth metallocene cations $[(C_5Me_5)_2Ln][(\mu\text{-}Ph)_2BPh_2]$ (Ln = Y, **1**; Sm, **2**) has been investigated with substrates that undergo reduction with f element complexes to probe metal-substrate interactions prior to reduction. Results with NaN_3, 1-adamantyl azide, acetone, benzophenone, phenanthroline, pyridine, azobenzene, and phenazine are described. Not only were coordination complexes isolated, but substrate reduction by $(BPh_4)^-$ was also observed. Complex **1** reacts with NaN_3 to form the azide $[(C_5Me_5)_2YN_3]_x$, **3**, which crystallizes as $[(C_5Me_5)_2Y(\mu\text{-}N_3)]_3$, **4**, when obtained from **1** and 1-adamantyl azide. The samarium analogue $[(C_5Me_5)_2SmN_3]_x$, **5**, can be produced similarly from **2** and NaN_3 and crystallized from MeCN as $[(C_5Me_5)_2Sm(NCMe)(\mu\text{-}N_3)]_3$, **6**, and $\{[(C_5Me_5)_2Sm(\mu\text{-}N_3)][(C_5Me_5)_2Sm(NCMe)(\mu\text{-}N_3)]\}_n$, **7**. Complexes **1** and **2** react with stoichiometric amounts of acetone and benzophenone to form the ketone adducts $[(C_5Me_5)_2Ln(OCMe_2)_2][BPh_4]$ (Ln = Y, **8**; Sm, **9**) and $[(C_5Me_5)_2Ln(OCPh_2)_2][BPh_4]$ (Ln = Y, **10**; Sm, **11**), respectively. Phenanthroline (phen) coordinates to **1** to form $[(C_5Me_5)_2Y(phen)][BPh_4]$, **12**. Complexes **1** and **2** react with pyridine (py) to form $[(C_5Me_5)_2Ln(py)_2][BPh_4]$, (Ln = Y, **13**; Sm, **14**). Complexes **3**, **8**, **10**, and **12** can also be made from the solvated cation $[(C_5Me_5)_2Y(THF)_2][BPh_4]$. The reaction of **1** with PhNNPh yields the diamagnetic adduct $[(C_5Me_5)_2Y(PhNNPh)][BPh_4]$, **15**, which transforms in benzene to the radical anion complex $(C_5Me_5)_2Y(PhNNPh)$, **16**, via a one electron reduction by $(BPh_4)^-$. Complex **1** similarly reacts with phenazine (phz) to produce the first rare earth phenazine radical anion complex $\{[(C_5Me_5)_2Y]_2(phz)\}\{BPh_4\}$, **17**. Further reduction of phenazine by $(BPh_4)^-$ in **17** yields $[(C_5Me_5)_2Y]_2(phz)$, **18**, which contains the common $(phz)^{2-}$ dianion. The reduction of fluorenone by $(BPh_4)^-$ is also reported.

INTRODUCTION

The unsolvated metallocene tetraphenylborate salts, $[(C_5Me_5)_2M][(\mu\text{-}Ph)_2BPh_2]$ (M = lanthanides,[1,2] Y,[2] U[3]), are highly reactive precursors to f element complexes that have expanded our knowledge in fundamental areas such as sterically induced reduction,[4] C−H bond activation,[2,5−7] and multielectron reduction via metal- and ligand-based processes.[8−10] For example, these complexes provide facile access to unsolvated alkyl complexes, $(C_5Me_5)_2LnR$,[5−7] eq 1, that are highly reactive in C−H bond activation. The $[(C_5Me_5)_2Ln][(\mu\text{-}Ph)_2BPh_2]$ complexes also provide one of the primary routes to the sterically crowded tris(pentamethylcyclopentadienyl) complexes, $(C_5Me_5)_3Ln$,[1,2,4] via reactions with KC_5Me_5, eq 2.

In contrast, the reaction of KC_5Me_5 with the tetrahydrofuran (THF)-solvated analogue, $[(C_5Me_5)_2M(THF)_2][BPh_4]$, forms ring-opened products, $(C_5Me_5)_2M[(O(CH_2)_4(C_5Me_5)](THF)$.[1,11,12] The latter reaction is thought to occur because the THF ligands are strongly activated by the Ln^{3+} center for nucleophilic attack. In the unsolvated $[(C_5Me_5)_2M][(\mu\text{-}Ph)_2BPh_2]$ complexes, the metallocene is only loosely ligated with the tetraphenylborate ion via long M···HC(aryl) interactions.

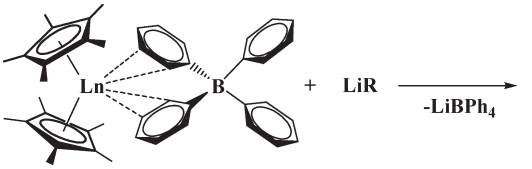

(1)

Ln = La, Sm, Lu
R = Me, CH_2SiMe_3, CH_2CMe_3

Received: January 7, 2011
Published: March 25, 2011

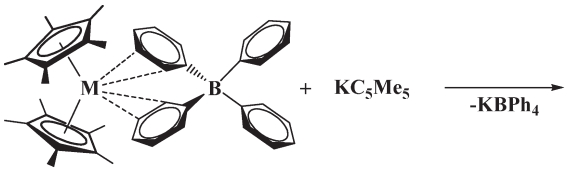

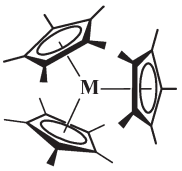

(2)

M = La, Ce, Pr, Nd, Sm, Gd, U

Because of the ease of displacement of the $(BPh_4)^-$ group in the $[(C_5Me_5)_2M][(\mu\text{-}Ph)_2BPh_2]$ complexes, they seemed to be ideal for investigating the initial interaction between metallocene cations and substrates. As part of our study of f element reduction, we have examined the reactions of these unsolvated metallocene cations with substrates that previously have been reduced by f element metallocene reductants such as $(C_5Me_5)_2Sm$,[13−16] $[(C_5Me_5)_2Ln]_2(\mu\text{-}\eta^2\text{:}\eta^2\text{-}N_2)$,[17,18] and the U^{3+} complex $[(C_5Me_5)_2U][(\mu\text{-}Ph)_2BPh_2]$.[8,19] Displacement of the $(BPh_4)^-$ counter-anions by the substrate could provide $[(C_5Me_5)_2Ln(substrate)_x][BPh_4]$ complexes that would reveal how these species bind to the metallocene prior to reduction. Reactions with the THF-solvated analogues, $[(C_5Me_5)_2M(THF)_2][BPh_4]$, were also examined for comparison.

A broad range of substrates previously shown to be reduced in f element based reduction systems was examined. These include PhN=NPh,[8,17,20−24] phenazine,[4,14,17,18,25−28] benzophenone,[29,30] phenanthroline,[31] pyridine,[32] and fluorenone.[29,30,33,34] Acetone was also included in the study for comparison with benzophenone.

Inorganic azides were also examined as substrates in light of the reduction of NaN_3 by $[(C_5Me_5)_2U][(\mu\text{-}Ph)_2BPh_2]$ to form the azide-nitride oligomer, $[(C_5Me_5)_2U(\mu\text{-}N)U(\mu\text{-}N_3)(C_5Me_5)_2]_4$.[19] This reaction presumably proceeds through a "$(C_5Me_5)_2UN_3$" intermediate, but such a species was not isolated with uranium. With a nonredox active Ln^{3+} ion, such an intermediate should be isolable by this cation route. The existence of the La^{3+} azide complex, $\{(C_5Me_5)_2La[CNN(SiMe_3)_2](\mu\text{-}N_3)\}_3$,[35] and the Sm^{3+} azide complex, $\{Li(DME)_3\}\{[(C_5H_5)_3Sm]_2(\mu\text{-}N_3)\}$,[36] suggested that this was viable.

This study focused on $[(C_5Me_5)_2Y][(\mu\text{-}Ph)_2BPh_2]$, **1**, and $[(C_5Me_5)_2Sm][(\mu\text{-}Ph)_2BPh_2]$, **2**. Complex **1** was chosen since Y^{3+} is diamagnetic and has a nuclear spin of $I = {}^1/_2$ that assists in making NMR and EPR assignments. Complex **2** was chosen because of the extensive reductive chemistry of $(C_5Me_5)_2Sm$ and the significant knowledge base that exists on the trivalent $(C_5Me_5)_2SmX$ products. These two metals also represent medium- and small-sized trivalent lanthanides[37] so that reactivity can also be examined as a function of metal size.

We report the new coordination complexes isolated from these reactions as well as reduction chemistry for the $(BPh_4)^-$ anion. Although the redox reactivity of $(BPh_4)^-$ has been known for decades,[38−46] eq 3, it has only recently been

$$(BPh_4)^- \rightarrow BPh_3 + 1/2Ph_2 + e^- \qquad (3)$$

found to be a useful method to enhance reductive reactivity in f element complexes. In reactions of $[(C_5Me_5)_2U][(\mu\text{-}Ph)_2BPh_2]$[8] and $[(C_5Me_5)Sm][(\mu\text{-}Ph)_2BPh_2]$,[25] the $(BPh_4)^-$ reduction combines with a metal-based reduction to give multielectron redox. Here we report that a redox active metal is not needed to effect reduction by $(BPh_4)^-$ in rare earth metal compounds.

EXPERIMENTAL SECTION

The syntheses and manipulations described below were conducted under nitrogen with rigorous exclusion of air and water using Schlenk, vacuum line, and glovebox techniques. Solvents were sparged with argon and dried over columns containing Q-5 and molecular sieves. NMR solvents were dried over NaK alloy, degassed by three freeze−pump−thaw cycles, and vacuum transferred before use. Acetone (Fisher) and pyridine (Aldrich) were dried over molecular sieves and degassed by three freeze−pump−thaw cycles before use. NaN_3, 1-adamantyl azide, PhNNPh, phenanthroline, fluorenone, and Ph_2CO were purchased from Aldrich and placed under 10^{-3} Torr for 12 h before use. Phenazine was purchased from Aldrich and sublimed before use. The unsolvated metallocene cation complexes $[(C_5Me_5)_2Ln][(\mu\text{-}Ph)_2BPh_2]$ (Ln = Y,[2] **1**; Sm,[1] **2**) were prepared as previously described. ^1H, ^{13}C, and ^{11}B NMR spectra were obtained on a Bruker DRX 500 MHz spectrometer at 25 °C, unless otherwise specified. ^{11}B NMR resonances were referenced with $BF_3\cdot Et_2O$ (δ = 0 ppm) as an external standard, and the presence of BPh_3 was associated with a ^{11}B NMR resonance at 68 ppm.[47] IR samples were prepared as KBr pellets, and the spectra were obtained on a Varian 1000 FT-IR spectrophotometer. Elemental analyses were performed with a Perkin-Elmer 2400 Series II CHNS analyzer. Electrospray ionization mass spectrometry (ESI-MS) spectra were obtained from a Waters (Micromass) LCT Premier orthogonal time-of-flight mass spectrometer. Electron paramagnetic resonance (EPR) spectra were collected using a Bruker EMX spectrometer equipped with an ER041XG microwave bridge. The magnetic field was calibrated with DPPH, and all experiments were conducted at room temperature. EPR spectra were simulated using the PEST WinSIM program.[48]

$[(C_5Me_5)_2YN_3]_x$, 3. NaN_3 (8 mg, 0.1 mmol) was stirred in THF (10 mL) for 10 min and then combined with a solution of $[(C_5Me_5)_2Y][(\mu\text{-}Ph)_2BPh_2]$, **1** (83 mg, 0.12 mmol) in THF (10 mL). The reaction mixture was allowed to stir for 24 h. The resulting white slurry was centrifuged, and the colorless supernatant was discarded. The white insoluble product was washed twice with THF and dried under vacuum to yield **3** as a white powder (43 mg, 88%). ^{1}H NMR (CD_3CN): δ 1.90 (br s, C_5Me_5, 30H). ^{13}C NMR (CD_3CN): δ 116.5 (C_5Me_5), 11.0 (C_5Me_5). IR: 3532w, 3391w, 2972s, 2909s, 2861s, 2726w, 2164vs, 2116vs, 1493m, 1439s, 1384m, 1165w, 1061m, 1022m, 729w, 639 m, 606w cm^{-1}. Anal. Calcd for $C_{20}H_{30}N_3Y$: C, 59.85; H, 7.53; N, 10.47. Found: C, 59.33; H, 7.25; N, 10.30. MS (ESI, MeCN) m/z (rel intensity): 443.1 (100) $\{[(C_5Me_5)_2Y(N_3)](N_3)\}^-$, 844.2 (68) $\{[(C_5Me_5)_2Y(N_3)]_2(N_3)\}^-$, 1245.4 (28) $\{[(C_5Me_5)_2Y(N_3)]_3(N_3)\}^-$, 1646.5 (9) $\{[(C_5Me_5)_2Y(N_3)]_4(N_3)\}^-$.

$[(C_5Me_5)_2Y(\mu\text{-}N_3)]_3$, 4. A solution of 1-adamantyl azide (15 mg, 0.085 mmol) in benzene (1 mL) was added to a slurry of **1** (59 mg, 0.087 mmol) in benzene (1 mL). The mixture immediately became a yellow solution. After 3 d at room temperature, colorless crystals of **4** suitable for X-ray diffraction were deposited from the reaction mixture (30 mg, 88%). The IR spectrum of these crystals was identical to that of the powder sample of **3** obtained above. The mother liquor was found to contain BPh_3 by ^{1}H and ^{11}B NMR spectroscopy. The mother liquor was passed through a column of silica gel to obtain a colorless solution. Analysis of the solution by GC-MS gave mass spectra consistent with the presence of C_5Me_5H and fragments of Ph_2 and adamantane.

$[(C_5Me_5)_2SmN_3]_x$, 5. Following the procedure for **3**, NaN_3 (6 mg, 0.09 mmol) was combined with $[(C_5Me_5)_2Sm][(\mu\text{-}Ph)_2BPh_2]$, **2**, (70 mg, 0.095 mmol) to yield **5** as a yellow powder (29 mg, 68%). ^{1}H NMR (CD_3CN): δ 1.17 (br s, C_5Me_5, 30H). ^{13}C NMR (CD_3CN): δ 112.9 (C_5Me_5), 16.7 (C_5Me_5). IR: 3495w, 2970s, 2908s, 2860s, 2726w,

dx.doi.org/10.1021/ic2000409 |Inorg. Chem. 2011, 50, 4092–4106

2142vs, 2097vs, 1494w, 1438s, 1385m, 1163w, 1061m, 1022m, 801w, 729w, 639m, 610m cm^{-1}. Anal. Calcd for $C_{20}H_{30}N_3Sm$: C, 51.90; H, 6.53; N, 9.08. Found: C, 51.81; H, 6.43; N, 9.08. MS (ESI, MeCN) *m/z* (rel intensity): 506.2 (100) $\{[(C_5Me_5)_2Sm(N_3)](N_3)\}^-$, 967.3 (28) $\{[(C_5Me_5)_2Sm(N_3)]_2(N_3)\}^-$, 1429.6 (8) $\{[(C_5Me_5)_2Sm(N_3)]_3(N_3)\}^-$, 1894.9 (8) $\{[(C_5Me_5)_2Sm(N_3)]_4(N_3)\}^-$.

$[(C_5Me_5)_2Sm(NCMe)(\mu\text{-}N_3)]_3$, 6. Yellow X-ray quality crystals of **6** were grown from a saturated solution of **5** in acetonitrile at −30 °C. When the mother liquor was removed and the crystals were allowed to dry by evaporation, they became dull and dark yellow in color. These dried solids were indistinguishable from **5** when analyzed by ^{1}H NMR and IR spectroscopy.

$\{[(C_5Me_5)_2Sm(\mu\text{-}N_3)][(C_5Me_5)_2Sm(NCMe)(\mu\text{-}N_3)]\}_n$, 7. Yellow X-ray quality crystals of **7** were grown over 3 d by allowing a concentrated solution of **5** in hot acetonitrile to cool slowly to room temperature. The IR spectrum of these crystals was identical to that of crude **5** isolated as a powder, except that an additional shoulder was observed at 2090 cm^{-1} in the azide stretching region.

$[(C_5Me_5)_2Y(OCMe_2)_2][BPh_4]$, 8. A 100 mL Schlenk flask was charged with a solution of **1** (70 mg, 0.10 mmol) in benzene (20 mL) in the glovebox and transferred to a Schlenk line. The flask was connected via a T-joint to another 100 mL Schlenk flask containing a 10:1 benzene/acetone mixture (20 mL). Under a static atmosphere of dinitrogen, both flasks were opened to allow slow diffusion of acetone into the solution of **1**. Over 2 d, light yellow needle-like crystals formed in the colorless solution. The crystals were collected by filtration, washed with benzene and hexane, and dried under vacuum to obtain **8** (74 mg, 91%). ^{1}H NMR (THF-d_8): δ 7.32 (br s, *o*-BPh_4, 8H), 6.88 (t, $^3J_{HH}$ = 7.0 Hz, *m*-BPh_4, 8H), 6.74 (t, $^3J_{HH}$ = 7.0 Hz, *p*-BPh_4, 4H), 2.24 (s, Me_2CO, 12H), 1.85 (s, C_5Me_5, 30H). ^{13}C NMR (THF-d_8): δ 204.3 (Me_2CO), 165.4 (BPh_4), 137.4 (BPh_4), 126.0 (BPh_4), 122.1 (BPh_4), 119.9 (C_5Me_5), 32.5 (Me_2CO), 11.2 (C_5Me_5). IR: 3055s, 2984s, 2906s, 2863s, 1942w, 1881w, 1814w, 1772w, 1678vs, 1581s, 1480s, 1427s, 1370s, 1247s, 1183m, 1148m, 1067m, 1031m, 914w, 848m, 734vs, 706vs, 613s cm^{-1}. Anal. Calcd for $C_{50}H_{62}BO_2Y$: C, 75.56; H, 7.86. Found: C, 75.16; H, 7.42. MS (ESI, THF) *m/z* (rel intensity): 359.1 (26) $[(C_5Me_5)_2Y]^+$, 417.2 (100) $[(C_5Me_5)_2Y(OCMe_2)]^+$, 431.2 (97) $[(C_5Me_5)_2Y(THF)]^+$, 489.2 (3) $[(C_5Me_5)_2Y(OCMe_2)(THF)]^+$.

$[(C_5Me_5)_2Y(OCMe_2)_2][BPh_4]$, 8, from $[(C_5Me_5)_2Y(THF)_2][BPh_4]$ and Acetone. Two equivalents of acetone were vacuum transferred to a frozen (−196 °C) colorless solution of $[(C_5Me_5)_2Y(THF)_2][BPh_4]$ prepared from **1** (10 mg, 0.015 mmol) in THF-d_8 (0.5 mL) in a J-Young NMR tube. The reaction mixture was warmed to room temperature and over 15 min turned pale yellow. Complex **8** was observed by ^{1}H NMR spectroscopy as the only product.

$[(C_5Me_5)_2Sm(OCMe_2)_2][BPh_4]$, 9. As described for **8**, acetone was allowed to diffuse slowly into a solution of **2** (55 mg, 0.070 mmol) in benzene (6 mL) yielding red orange needle-like crystals. The crystals were washed with benzene and hexane and dried under vacuum to obtain **9** (55 mg, 91%). ^{1}H NMR (THF-d_8): δ 7.17 (br s, *o*-BPh_4, 8H), 6.79 (t, $^3J_{HH}$ = 7.0 Hz, *m*-BPh_4, 8H), 6.68 (t, $^3J_{HH}$ = 7.0 Hz, *p*-BPh_4, 4H), 1.18 (s, Me_2CO, 12H), 0.77 (s, C_5Me_5, 30H). ^{13}C NMR (THF-d_8): δ 217.1 (Me_2CO), 165.2 (BPh_4), 137.2 (BPh_4), 125.8 (BPh_4), 122.0 (BPh_4), 118.1 (C_5Me_5), 30.2 (Me_2CO), 18.5 (C_5Me_5). IR: 3054s, 2984s, 2906s, 2861s, 1942w, 1880w, 1814w, 1772w, 1676vs, 1581s, 1480s, 1427s, 1370s, 1246s, 1183m, 1148m, 1067m, 1031m, 914w, 847m, 734vs, 706vs, 606s cm^{-1}. Anal. Calcd for $C_{50}H_{62}BO_2Sm$: C, 70.14; H, 7.30. Found: C, 69.45; H, 7.28. MS (ESI, THF) *m/z* (rel intensity): 422.1 (22) $[(C_5Me_5)_2Sm]^+$, 480.2 (33) $[(C_5Me_5)_2Sm(OCMe_2)]^+$, 494.2 (100) $[(C_5Me_5)_2Sm(THF)]^+$, 552.2 (5) $[(C_5Me_5)_2Sm(OCMe_2)(THF)]^+$.

$[(C_5Me_5)_2Y(OCPh_2)_2][BPh_4]$, 10. A solution of **1** (72 mg, 0.11 mmol) in benzene (10 mL) was added to a stirred solution of benzophenone (34 mg, 0.19 mmol) in benzene (4 mL). The combined solution immediately became red, and after 15 min of stirring the red slurry was centrifuged and the supernatant discarded. The insoluble material was washed with benzene and hexane and dried under vacuum to yield **10** as a red orange powder (84 mg, 86%). When the reaction mixture was filtered immediately after combining reagents and layered with hexane, slow evaporation over 5 d yielded X-ray quality crystals. ^{1}H NMR (THF-d_8, 5 °C): δ 7.78 (d, $^3J_{HH}$ = 7.5 Hz, *o*-Ph_2CO, 8H), 6.64 (br s, *m*-Ph_2CO, 4H), 7.60 (t, $^3J_{HH}$ = 7.5 Hz, *m*-Ph_2CO, 4H), 7.50 (t, $^3J_{HH}$ = 7.5 Hz, *p*-Ph_2CO, 4H), 7.30 (m, *o*-BPh_4, 8H), 6.86 (t, $^3J_{HH}$ = 7.0 Hz, *m*-BPh_4, 8H), 6.72 (t, $^3J_{HH}$ = 7.0 Hz, *p*-BPh_4, 4H), 1.92 (s, C_5Me_5, 30H). ^{13}C NMR (THF-d_8, 5 °C): δ 196.1 (Ph_2CO), 165.3 (BPh_4), 137.3 (BPh_4), 133.2 (Ph_2CO), 130.9 (Ph_2CO), 129.2 (Ph_2CO), 125.9 (BPh_4), 122.0 (BPh_4), 121.1 (C_5Me_5), 11.9 (C_5Me_5). ^{11}B NMR (THF-d_8, −70 °C): δ −5.99 (BPh_4). IR: 3055m, 3033m, 3000m, 2982m, 2941m, 2905m, 2859m, 2156w, 1939w, 1879w, 1819w, 1656w, 1603s, 1558s, 1480s, 1448s, 1381m, 1327s, 1294s, 1160s, 1078m, 1032m, 999s, 941s, 842s, 810m, 771s, 734s, 705s, 636s, 613s cm^{-1}. Anal. Calcd for $C_{70}H_{70}BO_2Y$: C, 80.61; H, 6.76. Found: C, 80.64; H, 6.91.

$[(C_5Me_5)_2Y(OCPh_2)_2][BPh_4]$, 10, from $[(C_5Me_5)_2Y(THF)_2][BPh_4]$ and Benzophenone. A solution of $[(C_5Me_5)_2Y(THF)_2][BPh_4]$ prepared from **1** (18 mg, 0.027 mmol) in THF (3 mL) was combined with a solution of benzophenone (12 mg, 0.067 mmol) in THF (1 mL). A red solution immediately formed, and the solvent was removed under vacuum. Analysis of the resulting tacky red residue by ^{1}H NMR spectroscopy showed residual Ph_2CO and **10** as the only organometallic product.

$[(C_5Me_5)_2Sm(OCPh_2)_2][BPh_4]$, 11. A solution of **2** (22 mg, 0.030 mmol) in benzene (5 mL) was added to a stirred solution of benzophenone (12 mg, 0.067 mmol) in benzene (5 mL). The maroon red solution quickly turned dark red and then to red orange. After 15 min of stirring, the red slurry was centrifuged and the supernatant discarded. The insoluble material was washed with benzene and hexane and dried under vacuum to yield **11** as a red orange powder (25 mg, 75%). ^{1}H NMR (THF-d_8, 5 °C): δ 7.54 (t, $^3J_{HH}$ = 7.5 Hz, *p*-Ph_2CO, 4H), 7.38 (br s, *o*/*m*-Ph_2CO, 16H), 7.20 (m, *o*-BPh_4, 8H), 6.83 (t, $^3J_{HH}$ = 7.0 Hz, *m*-BPh_4, 8H), 6.73 (t, $^3J_{HH}$ = 7.0 Hz, *p*-BPh_4, 4H), 0.92 (s, C_5Me_5, 30H). ^{13}C NMR (THF-d_8, 5 °C): δ 165.2 (BPh_4), 137.2 (BPh_4), 134.0 (Ph_2CO), 130.8 (Ph_2CO), 129.2 (Ph_2CO), 125.9 (BPh_4), 122.0 (BPh_4), 119.0 (C_5Me_5), 18.7 (C_5Me_5). The ^{13}C resonance for Ph_2CO was not located. ^{11}B NMR (THF-d_8, −70 °C): δ −6.06 (BPh_4). IR: 3055m, 3034m, 2982m, 2905m, 2859m, 2728w, 2332w, 2239w, 1940w, 1818w, 1759w, 1656w, 1603s, 1554s, 1480s, 1448s, 1426s, 1383m, 1326s, 1291s, 1180s, 1159s, 1077s, 1032s, 999s, 976m, 941s, 923s, 842s, 811m, 770s, 734s, 704s, 636s, 613 cm^{-1}. Anal. Calcd for $C_{70}H_{70}BO_2Sm$: C, 76.12; H, 6.39. Found: C, 76.00; H, 6.31.

$[(C_5Me_5)_2Y(phen)][BPh_4]$, 12. A solution of phenanthroline (10 mg, 0.055 mmol) in benzene (3 mL) was added to a stirred solution of **1** (36 mg, 0.053 mmol) in benzene (10 mL). The mixture immediately turned cloudy yellow. After 15 min, the insoluble material was obtained by centrifugation and removal of the supernatant. The solids were dried under vacuum to yield **12** as a bright yellow powder (43 mg, 94%). Crystals suitable for X-ray diffraction were grown over several days from a concentrated THF solution at −35 °C. ^{1}H NMR (THF-d_8, 5 °C): δ 8.47 (m, *phen*, 4H), 7.92 (s, *phen*, 2H), 7.81 (dd, *phen*, 2H), 7.40 (br s, *o*-BPh_4, 8H), 6.87 (t, $^3J_{HH}$ = 7.0 Hz, *m*-BPh_4, 8H), 6.72 (t, $^3J_{HH}$ = 7.0 Hz, *p*-BPh_4, 4H), 1.63 (s, C_5Me_5, 30H). ^{13}C NMR (THF-d_8, 5 °C): δ 165.4 (BPh_4), 150.2 (*phen*), 143.2 (*phen*), 142.8 (*phen*), 137.4 (BPh_4), 131.7 (*phen*), 129.5 (*phen*), 126.4 (*phen*), 126.1 (BPh_4), 122.3 (BPh_4), 120.3 (C_5Me_5), 11.0 (C_5Me_5). ^{11}B NMR (THF-d_8, −70 °C): δ −5.96 (BPh_4). IR: 3056m, 3035m, 2907m, 2860m, 2730w, 1944w, 1881w, 1819w, 1764w, 1625m, 1580m, 1523s, 1479s, 1425s, 1380 m, 1340w, 1301w, 1266m, 1221w, 1184w, 1146m, 1105m, 1065w, 1032 m, 912w, 849s, 803w, 777w, 731s, 705s, 682s, 644 m, 613s, 509w cm^{-1}. Anal. Calcd for $C_{56}H_{58}BN_2Y$: C, 78.32; H, 6.81; N, 3.26. Found: C, 78.60; H, 6.89; N, 2.99.

[(C$_5$Me$_5$)$_2$Y(phen)][BPh$_4$], 12, from [(C$_5$Me$_5$)$_2$Y(THF)$_2$][BPh$_4$] and Phenanthroline. A solution of [(C$_5$Me$_5$)$_2$Y(THF)$_2$][BPh$_4$] prepared by dissolving **1** (26 mg, 0.038 mmol) in THF (3 mL) was combined with a solution of phenanthroline (7 mg, 0.04 mmol) in THF (1 mL). A yellow solution immediately formed, and the solvent was removed under vacuum. Analysis of the resulting tacky yellow residue by ^{1}H NMR spectroscopy showed residual phenanthroline and **12** as the only organometallic product.

[(C$_5$Me$_5$)$_2$Y(py)$_2$][BPh$_4$], 13. Pyridine (24 mg, 0.30 mmol) was diluted with benzene (5 mL) and was added to a stirred solution of **1** (74 mg, 0.11 mmol) in benzene (7 mL). A white precipitate immediately formed. After stirring for 15 min, the reaction mixture was centrifuged and the supernatant removed. The solids were washed with benzene and hexane and dried under vacuum to yield **13** as a white powder (71 mg, 77%). The ^{1}H NMR spectrum of **13** in THF-d_8 showed three (C$_5$Me$_5$)$^-$ resonances, one of which was attributed to [(C$_5$Me$_5$)$_2$Y(THF)$_2$][BPh$_4$] at 1.92 ppm, and several sets of pyridine peaks, including free pyridine. ^{1}H NMR (pyridine-d_5): δ 8.15 (br s, *o*-BP*h*$_4$, 8H), 7.35 (t, $^3J_{HH}$ = 7.0 Hz, *m*-BP*h*$_4$, 8H), 7.17 (t, $^3J_{HH}$ = 7.0 Hz, *p*-BP*h*$_4$, 4H), 1.67 (s, C$_5$*Me*$_5$, 30H). The ^{1}H and ^{13}C resonances of the pyridine ligands were not observed because of exchange with pyridine-d_5. ^{13}C NMR (pyridine-d_5): δ 165.5 (B*Ph*$_4$), 137.6 (B*Ph*$_4$), 126.1 (B*Ph*$_4$), 122.8 (B*Ph*$_4$), 120.9 (*C*$_5$Me$_5$), 11.0 (C$_5$*Me*$_5$). ^{11}B NMR (pyridine-d_5): δ −5.96 (*B*Ph$_4$). IR: 3055m, 2983m, 2908m, 2862m, 2731w, 2472w, 1942w, 1884w, 1817w, 1764w, 1702w, 1638w, 1602s, 1580s, 1480s, 1441s, 1381m, 1307w, 1267m, 1217s, 1182m, 1158m, 1067s, 1030s, 1008s, 948m, 915w, 846s, 802w, 733s, 708s, 614s cm^{-1}. Anal. Calcd for C$_{54}$H$_{60}$BN$_2$Y: C, 77.51; H, 7.23; N, 3.35. Found: C, 76.98; H, 7.55; N, 3.32.

[(C$_5$Me$_5$)$_2$Sm(py)$_2$][BPh$_4$], 14. As described for **13**, pyridine (17 mg, 0.21 mmol) was combined with **2** (50 mg, 0.068 mmol) to produce an orange reaction mixture, from which **14** was isolated as a light orange powder (41 mg, 67%). X-ray quality crystals of **14** were grown by slow diffusion of pyridine into a benzene solution of **2** over 4 d. The ^{1}H NMR spectrum of **14** in THF-d_8 showed [(C$_5$Me$_5$)$_2$Sm(THF)$_2$][BPh$_4$][11] as the major component and several sets of pyridine peaks, including free pyridine. ^{1}H NMR (pyridine-d_5): δ 8.11 (br s, *o*-BP*h*$_4$, 8H), 7.33 (t, $^3J_{HH}$ = 7.0 Hz, *m*-BP*h*$_4$, 8H), 7.16 (t, $^3J_{HH}$ = 7.0 Hz, *p*-BP*h*$_4$, 4H), 0.87 (s, C$_5$*Me*$_5$, 30H). The ^{1}H and ^{13}C resonances of the pyridine ligands were not observed because of exchange with pyridine-d_5. ^{13}C NMR (pyridine-d_5): δ 165.6 (B*Ph*$_4$), 137.6 (B*Ph*$_4$), 126.1 (B*Ph*$_4$), 122.8 (B*Ph*$_4$), 118.5 (*C*$_5$Me$_5$), 17.9 (C$_5$*Me*$_5$). ^{11}B NMR (pyridine-d_5): δ −5.64 (*B*Ph$_4$). IR: 3055m, 2983m, 2907m, 2860m, 2731w, 2361w, 1944w, 1884w, 1818w, 1767w, 1635w, 1600s, 1580m, 1479s, 1441s, 1384m, 1267m, 1217m, 1182m, 1158m, 1068s, 1041m, 1007s, 946w, 915w, 846 m, 802w, 733s, 704s, 606s cm^{-1}. Anal. Calcd for C$_{54}$H$_{60}$BN$_2$Sm: C, 72.21; H, 6.73; N, 3.12. Found: C, 71.96; H, 6.80; N, 3.08.

[(C$_5$Me$_5$)$_2$Y(PhNNPh)][BPh$_4$], 15. PhN═NPh (4.2 mL of a 0.023 M solution in methylcyclohexane, 0.097 mmol) was added via syringe to a slurry of **1** (65 mg, 0.096 mmol) in methylcyclohexane (15 mL). After 42 h, the orange mixture had turned brown, and the brown solids were collected by centrifugation, washed twice with benzene and twice with hexane, and dried under vacuum to yield **15** as a fine brown powder (40 mg, 48%). ^{1}H NMR (C$_6$D$_6$): δ 8.10 (br s, N*Ph*, 10H), 7.67 (d, $^3J_{HH}$ = 5.5 Hz, *o*-BP*h*$_4$, 8H), 7.32 (m, $^3J_{HH}$ = 5.5, 7.0 Hz, *m*-BP*h*$_4$, 8H), 7.25 (t, $^3J_{HH}$ = 7.0 Hz, *p*-BP*h*$_4$, 4H), 1.59 (s, C$_5$*Me*$_5$, 30H); (THF-d_8, −70 °C): δ 7.60 (m, N*Ph*, 1H), 7.53 (m, N*Ph*, 2H), 7.51 (br s, N*Ph*, 2H), 7.34 (s, N*Ph*, 2H), 7.28 (t, $^3J_{HH}$ = 8.0 Hz, N*Ph*, 1H), 7.25 (br s, *o*-BP*h*$_4$, 8H), 7.15 (t, $^3J_{HH}$ = 7.5 Hz, N*Ph*, 1H), 6.86 (t, $^3J_{HH}$ = 7.5 Hz, *m*-BP*h*$_4$, 8H), 6.83 (m, N*Ph*, 1H), 6.73 (t, $^3J_{HH}$ = 7.0 Hz, *p*-BP*h*$_4$, 4H), 1.91 (s, C$_5$*Me*$_5$, 30H). ^{13}C NMR (THF-d_8, −70 °C): δ 164.9 (B*Ph*$_4$), 154.7 (N*Ph*), 150.0 (N*Ph*), 137.1 (B*Ph*$_4$), 136.0 (N*Ph*), 132.8 (N*Ph*), 132.2 (N*Ph*), 131.1 (N*Ph*), 129.7 (N*Ph*), 127.9 (N*Ph*), 127.1 (N*Ph*), 125.8 (B*Ph*$_4$), 122.0 (B*Ph*$_4$), 121.3 (N*Ph*), 120.9 (N*Ph*), 119.6 (*C*$_5$Me$_5$), 12.0 (C$_5$*Me*$_5$). ^{11}B NMR (C$_6$D$_6$): δ −5.85 (*B*Ph$_4$); (THF-d_8, −70 °C): −6.07 (*B*Ph$_4$). MS (ESI, C$_6$H$_6$) *m*/*z* (rel intensity): 359.1 (20) [(C$_5$Me$_5$)$_2$Y]$^+$, 541.2 (100) [(C$_5$Me$_5$)$_2$Y(PhNNPh)]$^+$; 319.2 (100) [BPh$_4$]$^-$. IR: 3600w, 3056m, 3034m, 2985m, 2909m, 2861m, 2732w, 1938w, 1876w, 1810w, 1760w, 1581s, 1479s, 1440s, 1382m, 1316w, 1268w, 1164m, 1066m, 1032m, 999m, 938w, 902w, 846m, 772s, 730vs, 703vs, 680s, 606s, 518w cm^{-1}. Anal. Calcd for C$_{56}$H$_{60}$BN$_2$Y: C, 78.14; H, 7.03; N, 3.25. Found: C, 77.15; H, 6.86; N, 3.02.

(C$_5$Me$_5$)$_2$Y(PhNNPh), 16. A dark brown suspension of **15** (112 mg, 0.128 mmol, from several preparations as described above) in benzene (15 mL) was heated at reflux for 1 h, during which time it became a green solution. The solvent was removed under vacuum to yield a tacky mixture of green and colorless solids. Extraction of this mixture with hexane and removal of solvent gave an oily green residue containing **16**. Complex **16** is NMR silent, but the green oil was found to contain BPh$_3$ and Ph$_2$ by ^{1}H and ^{11}B NMR spectroscopy. MS (ESI, hexane) *m*/*z* (rel intensity): 541.2 (100) [(C$_5$Me$_5$)$_2$Y(PhNNPh)]$^+$. EPR (hexane): g = 2.004; a_N = 8.25 G (2N); a_H = 2.40 G (6H), 0.95 G (4H); a_Y = 1.95 G (1Y).

{[(C$_5$Me$_5$)$_2$Y]$_2$(phz)}{BPh$_4$}, 17. Phenazine (7 mg, 0.04 mmol) and **1** (52 mg, 0.077 mmol) were combined in benzene (10 mL) and stirred for 2 d, during which time the amber solution turned dark green. After the solvent was removed under vacuum, the brown tacky solids were washed with hexane and dried under vacuum. The solids were dissolved in hot benzene (4 mL), and hexane was slowly diffused into the solution over 2 d to yield **17** as dark green X-ray quality crystals (35 mg, 74%). When the reaction was monitored by ^{1}H NMR spectroscopy in C$_6$D$_6$, the resonances of the starting materials gradually diminished and resonances for BPh$_3$ and Ph$_2$ grew in. Complex **17** is NMR silent as there were no resonances attributable to (C$_5$Me$_5$)$^-$ or (phz)$^-$ in the ^{1}H NMR spectrum. EPR (benzene): g = 2.005; a_N = 5.44 G (2N); a_H = 1.68 G (4H), 0.95 G (4H); a_Y = 1.18 G (2Y). IR: 3033m, 2965m, 2909m, 2861m, 1935w, 1876w, 1813w, 1759w, 1655w, 1604m, 1579m, 1532m, 1480m, 1429m, 1381m, 1326s, 1261m, 1185w, 1153m, 1064m, 1031m, 901s, 824m, 800w, 732s, 703s, 679s, 613s cm^{-1}. Anal. Calcd for C$_{76}$H$_{92}$BN$_2$Y: C, 74,69; H, 7.59; N, 2.29. Found: C, 74.93; H, 7.48; N, 2.19.

[(C$_5$Me$_5$)$_2$Y]$_2$(phz), 18. A solution of **17** (15 mg, 0.012 mmol) in C$_6$D$_6$ (0.5 mL) was sealed in a J-Young NMR tube and heated at 70 °C over 2 d. The dark green solution slowly turned red and two different diamagnetic phenazine-containing products were identified along with BPh$_3$, Ph$_2$, and 5,10-dihydrophenazine (phzH$_2$) in the ^{1}H NMR spectrum. The assignments of 5,10-dihydrophenazine were confirmed by comparison to an independently synthesized sample.[49] Red crystals of **18** suitable for X-ray diffraction were grown at room temperature over several weeks via slow evaporation of an NMR sample of **17** in C$_6$D$_6$. ^{1}H NMR (C$_6$D$_6$): **18**, δ 6.07 (m, *phz*, 4H), 4.88 (m, *phz*, 4H), 2.11 (s, C$_5$*Me*$_5$, 60H); (C$_5$Me$_5$)$_2$Y(phzH), δ 6.24 (m, *phz*H, 4H), 5.42 (m, *phz*H, 2H), 4.94 (m, *phz*H, 2H), 3.74 (br s, phz*H*, 1H), 1.98 (s, C$_5$*Me*$_5$, 30H); phzH$_2$, δ 6.46 (m, *phz*H$_2$, 4H), 5.70 (m, *phz*H$_2$, 4H), 3.94 (br s, phz*H*$_2$, 2H).

Reaction of 1 with Fluorenone. A solution of fluorenone, C$_7$H$_8$O, (15 mg, 0.083 mmol) in benzene (5 mL) was added to a stirred solution of **1** (55 mg, 0.081 mmol) in benzene (5 mL). The mixture quickly became dark burgundy in color. After 20 min of stirring, the resulting precipitate was collected by centrifugation, washed with benzene, and dried under vacuum to yield a dark burgundy powder (34 mg). The supernatant contained unreacted **1** and BPh$_3$ when analyzed by ^{1}H and ^{11}B NMR spectroscopy. The solids were dissolved in THF-d_8, and both diamagnetic and paramagnetic species, consistent with [(C$_5$Me$_5$)$_2$Y(OC$_7$H$_8$)(THF)$_x$][BPh$_4$] and (C$_5$Me$_5$)$_2$Y(OC$_7$H$_8$)$_n$-(THF)$_x$ (n = 1, 2), respectively, were observed by ^{1}H, ^{13}C, and ^{11}B NMR and EPR spectroscopy. The EPR spectrum of the THF solution supports the formation of a fluorenone radical complex. ^{1}H NMR (THF-d_8, −70 °C): δ 7.76 (d, $^3J_{HH}$ = 7.5 Hz, C$_7$*H*$_8$O, 2H), 7.63 (d, $^3J_{HH}$ = 7.5 Hz,

Table 1. X-ray Data Collection Parameters for $[(C_5Me_5)_2Y(\mu\text{-}N_3)]_3$, 4, $[(C_5Me_5)_2Sm(NCMe)(\mu\text{-}N_3)]_3$, 6, $\{[(C_5Me_5)_2Sm(\mu\text{-}N_3)][(C_5Me_5)_2Sm(NCMe)(\mu\text{-}N_3)]\}_n$, 7, $[(C_5Me_5)_2Y(OCMe_2)_2][BPh_4]$, 8, and $[(C_5Me_5)_2Sm(OCMe_2)_2][BPh_4]$, 9

	4	6	7	8	9
empirical formula	$C_{60}H_{90}N_9Y_3$	$C_{66}H_{99}N_{12}Sm_3 \cdot 6(CH_3CN)$	$[C_{42}H_{63}N_7Sm_2]_\infty$	$C_{50}H_{62}BO_2Y$	$C_{50}H_{62}BO_2Sm$
fw	1204.14	1757.95	966.69	794.72	856.16
temp (K)	93(2)	148(2)	93(2)	93(2)	98(2)
crys syst	monoclinic	trigonal	triclinic	monoclinic	monoclinic
space group	*C*2/*c*	$P\bar{3}$	$P\bar{1}$	*P*2/*c*	*P*2/*c*
a (Å)	22.2813(8)	27.1898(15)	10.8241(4)	10.3246(4)	10.3283(3)
b (Å)	14.5879(6)	27.1898(15)	14.1064(5)	14.1253(6)	14.1678(5)
c (Å)	19.2893(7)	19.8371(11)	14.3236(5)	15.5657(7)	15.6546(5)
α (deg)	90	90	86.1256(4)	90	90
β (deg)	105.7323	90	79.4371(4)	105.1600(10)	105.3136(4)
γ (deg)	90	120	83.4938(4)	90	90
volume (Å^3)	6034.9(4)	12700.5(12)	2133.70(13)	2191.07(16)	2209.39(12)
Z	4	6	2	2	2
ρ_{calcd} (mg/m^3)	1.325	1.379	1.505	1.205	1.287
μ (mm^{-1})	2.905	2.103	2.761	1.368	1.366
R1[a] ($I > 2.0\sigma(I)$)	0.0247	0.0252	0.0236	0.0321	0.0155
wR2[b] (all data)	0.0642	0.0623	0.0564	0.0782	0.0389

[a] $R1 = \Sigma||F_o| - |F_c||/\Sigma|F_o|$. [b] $wR2 = [\Sigma w(F_o^2 - F_c^2)^2/\Sigma w(F_o^2)^2]^{1/2}$.

C_7H_8O, 2H), 7.60 (t, $^3J_{HH}$ = 7.5 Hz, C_7H_8O, 2H), 7.39 (t, $^3J_{HH}$ = 7.5 Hz, C_7H_8O, 2H), 7.28 (br s, *o*-B*Ph*$_4$, 8H), 6.88 (t, $^3J_{HH}$ = 7.5 Hz, *m*-B*Ph*$_4$, 8H), 6.75 (t, $^3J_{HH}$ = 7.5 Hz, *p*-B*Ph*$_4$, 4H), 1.92 (br s, C_5Me_5, 30H). ^{13}C NMR (THF-d_8, 5 °C): δ 165.4 (B*Ph*$_4$), 137.4 (B*Ph*$_4$), 125.9 (B*Ph*$_4$), 122.0 (C_5Me_5), 11.8 (C_5Me_5), the ^{13}C resonances of fluorenone could not be located. ^{11}B NMR (THF-d_8): δ −6.1 (B*Ph*$_4$). EPR (THF): g = 2.003; a_H = 3.36 G (2H), 0.73 G (2H), 2.76 G (2H), 0.61 G (2H); a_Y = 0.63 G (1Y).

X-ray Data Collection, Structure Determination, and Refinement. Crystallographic information for complexes **4**, **6**, **7**, **8**, **9**, **10**, **12**, **14**, **17**, and **18** is summarized in the Supporting Information and Tables 1 and 2.

RESULTS

Synthesis of Lanthanide Metallocene Azides. The reaction of **1** and **2** with 1 equiv of NaN_3 yields $[(C_5Me_5)_2LnN_3]_x$ (Ln = Y, **3**; Sm, **5**), eq 4. The reaction proceeds slowly in benzene, most likely because of the insolubility of NaN_3. The reaction time is greatly reduced when THF is used as the solvent and $[(C_5Me_5)_2Ln(THF)_2][BPh_4]$, formed in situ, is the starting material. Even in THF, the same unsolvated complexes, **3** and **5**, are isolated.

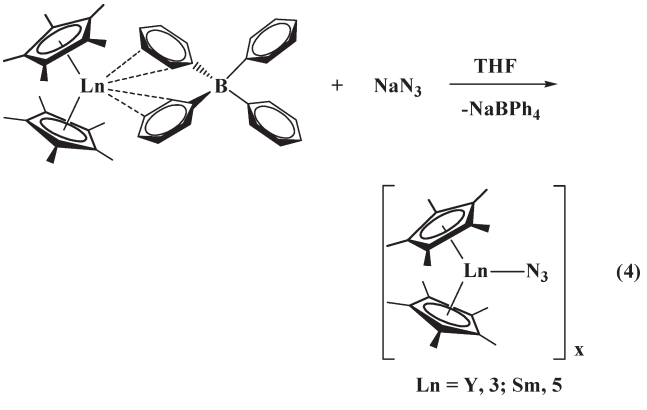

(4)

Ln = Y, 3; Sm, 5

Elemental analyses of **3** and **5** were consistent with their expected elemental compositions. The negative ESI-MS spectra of millimolar solutions of **3** and **5** in MeCN, Figure 1, show several mass peaks that correspond to the exact masses of mono-, bi-, tri-, and tetra-metallic species containing $(C_5Me_5)^-$ and $(N_3)^-$ ligands. Variable-temperature ^{1}H NMR studies of **5** in CD_3CN revealed only one $(C_5Me_5)^-$ resonance between −30 and 60 °C.

Analysis of these complexes by IR spectroscopy revealed two strong absorptions at 2164 and 2116 cm^{-1} for **3** and 2142 and 2097 cm^{-1} for **5**. These absorptions are in the region typical for the asymmetric stretch observed in coordinated azides.[50] These sharp absorption bands differ from the broad absorption band of NaN_3 at 2129 cm^{-1}, but are similar to the 2115 cm^{-1} band for $\{(C_5Me_5)_2La[CNN(SiMe_3)_2](\mu\text{-}N_3)\}_3$[35] and the 2111 and 2073 cm^{-1} bands for $[(C_5Me_5)_2U(N_3)(\mu\text{-}N_3)]_3$.[51] The presence of two azide stretches in each complex suggests that there are multiple azide sites in these solids.

A crystalline derivative of **5** was obtained from MeCN at −30 °C and was found to be the cyclic trimer $[(C_5Me_5)_2Sm(NCMe)(\mu\text{-}N_3)]_3$, **6**, by X-ray diffraction, Figure 2. The structure of **6** in the solid state has a 3-fold rotational axis down the center of the 12-membered ring, and the bridging azides are in the plane of the three metals. Similar arrangements of bridging azides are found in $\{(C_5Me_5)_2La[CNN(SiMe_3)_2](\mu\text{-}N_3)\}_3$[35] and $[(C_5Me_5)_2U(N_3)(\mu\text{-}N_3)]_3$.[51] In these complexes, as well as **6**, the metal is fully saturated with a formal coordination number of nine.

Complex **5** crystallized with only one MeCN per two samarium ions when a hot acetonitrile solution was allowed to cool to room temperature. X-ray diffraction revealed that these yellow crystals existed as a polymeric samarium azide chain, $\{[(C_5Me_5)_2Sm(\mu\text{-}N_3)][(C_5Me_5)_2Sm(NCMe)(\mu\text{-}N_3)]\}_n$, **7**. Figure 3 shows two repeat units of this polymer, in which the two crystallographically independent samarium positions are arranged $(Sm1-Sm1-Sm2-Sm2)_n$ rather than $(Sm1-Sm2-Sm1-Sm2)_n$. The equivalent metallocene units are symmetry related by inversion at N1 and

dx.doi.org/10.1021/ic2000409 |*Inorg. Chem.* 2011, 50, 4092–4106

Table 2. X-ray Data Collection Parameters for $[(C_5Me_5)_2Y(OCPh_2)_2][BPh_4]$, 10, $[(C_5Me_5)_2Y(phen)][BPh_4]$, 12, $[(C_5Me_5)_2Sm(py)_2][BPh_4]$, 14, $\{[(C_5Me_5)_2Y]_2(phz)\}\{BPh_4\}$, 17, and $[(C_5Me_5)_2Y]_2(phz)$, 18

	10	12	14	17	18
empirical formula	$C_{70}H_{70}BO_2Y$	$C_{64}H_{74}BN_2O_2Y$	$C_{54}H_{60}BN_2Sm$	$[C_{52}H_{68}N_2Y_2][C_{24}H_{20}B](C_6H_6)$	$C_{52}H_{68}N_2Y_2(C_6H_6)$
fw	1042.98	1002.97	898.20	1296.22	977.01
temp (K)	143(2)	143(2)	93(2)	93(2)	148(2)
crys syst	monoclinic	orthorhombic	monoclinic	orthorhombic	triclinic
space group	$P2_1/c$	$P2_12_12_1$	$P2/c$	$P2_12_12_1$	$P\bar{1}$
a (Å)	10.9624(5)	11.0392(5)	10.3569(4)	13.6157(5)	10.5327(5)
b (Å)	14.7189(7)	15.5736(8)	14.1863(5)	18.4964(7)	10.9558(5)
c (Å)	34.3027(17)	31.0265(15)	16.1998(6)	27.1343(10)	11.2847(5)
α (deg)	90	90	90	90	79.5057(6)
β (deg)	92.5507(7)	90	106.8571(4)	90	75.6293(6)
γ(deg)	90	90	90	90	85.1580(6)
volume (Å^3)	5529.4(5)	5334.1(4)	2277.90(15)	6833.5(4)	1239.29(10)
Z	4	4	2	4	1
ρ_{calcd} (mg/m^3)	1.253	1.249	1.310	1.260	1.309
μ (mm^{-1})	1.101	1.139	1.326	1.735	2.368
R1[a] ($I > 2.0\sigma(I)$)	0.0413	0.0400	0.0182	0.0335	0.0282
wR2[b] (all data)	0.0956	0.0980	0.0464	0.0729	0.0725

[a] $R1 = \Sigma||F_o| - |F_c||/\Sigma|F_o|$. [b] $wR2 = [\Sigma w(F_o^2 - F_c^2)^2/\Sigma w(F_o^2)^2]^{1/2}$.

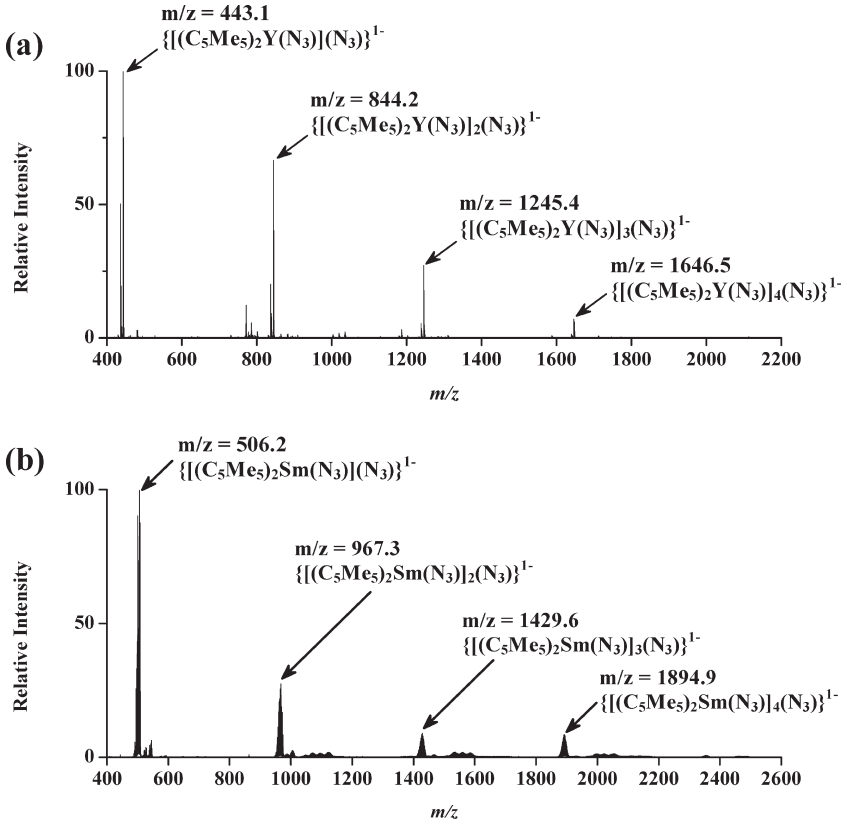

Figure 1. Negative ESI-MS spectra of (a) **3** and (b) **5** in MeCN. Mass peaks corresponding to $(BPh_4)^-$, $[Na(BPh_4)_2]^-$, and $[K(BPh_4)_2]^-$ ions were omitted for clarity.

N7. Complex **7** contains both solvated nine coordinate and unsolvated eight coordinate samarium centers.

Surprisingly, a crystalline *unsolvated* cyclic trimeric derivative of **3**, namely, $[(C_5Me_5)_2Y(\mu\text{-}N_3)]_3$, **4**, could also be isolated and characterized by X-ray diffraction, Figure 4. The crystals were obtained from the reaction of **1** with 1-adamantyl azide, eq 5, a reaction that involves reduction of the organic azide. Since the mother liquor contained BPh_3, identified by ^1H and ^{11}B NMR

dx.doi.org/10.1021/ic2000409 |*Inorg. Chem.* 2011, 50, 4092–4106

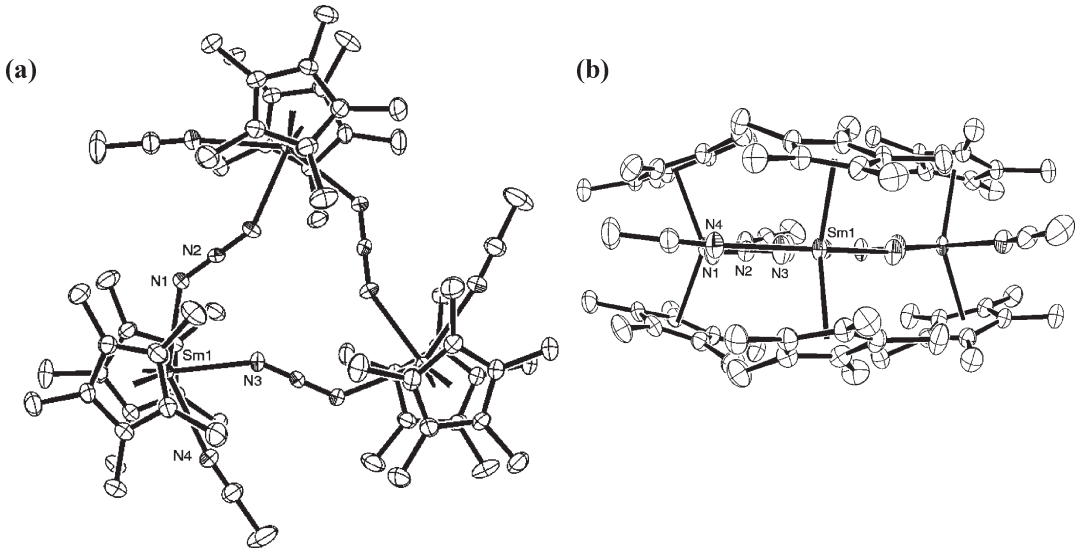

Figure 2. ORTEP[52] of $[(C_5Me_5)_2Sm(NCMe)(\mu\text{-}N_3)]_3$, **6**, shown at the 50% probability level from the (a) axial and (b) equatorial viewpoints. The hydrogen atoms have been omitted for clarity.

spectroscopy, and GC-MS analysis revealed peaks for adamantane, adamantylbenzene, and biphenyl, the $(BPh_4)^-$ anion was presumably the component that reduced 1-adamantyl azide according to eq 3. The IR spectrum of the crystals was identical to that of samples of **3** isolated as a powder. The solid-state structure of the unsolvated **4**, shown in Figure 4, has major differences from that of **6**. Complex **4** has a 2-fold rotational axis between Y1 and N5, and only the central nitrogen atoms of the bridging azides are in the trimetallic plane (within 0.06 Å).

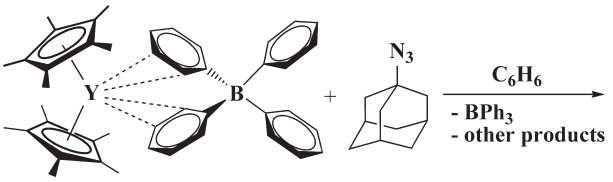

1

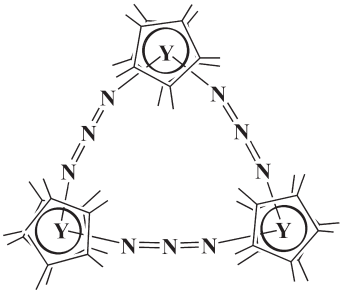

4 (5)

Structural Analysis of $[(C_5Me_5)_2Y(\mu\text{-}N_3)]_3$, 4, $[(C_5Me_5)_2Sm(NCMe)(\mu\text{-}N_3)]_3$, 6, and $\{[(C_5Me_5)_2Sm(\mu\text{-}N_3)][(C_5Me_5)_2Sm(NCMe)(\mu\text{-}N_3)]\}_n$, 7. Crystallographic data on **4**, **6**, and **7** are presented in Table 3 along with a comparison to $\{(C_5Me_5)_2La[CNN(SiMe_3)_2](\mu\text{-}N_3)\}_3$,[35] **19**. The Ln−($C_5Me_5$ ring centroid) and Ln−N(azide) distances in these complexes are all similar when the differences in ionic radii are considered: eight coordinate Y^{3+}, 1.019 Å; eight coordinate Sm^{3+}, 1.079 Å; nine coordinate Sm^{3+}, 1.132 Å; and nine coordinate La^{3+}, 1.216 Å.[37] The (C_5Me_5 ring centroid)−Ln−(C_5Me_5 ring centroid) angles are all very similar to each other and to other known examples.[53]

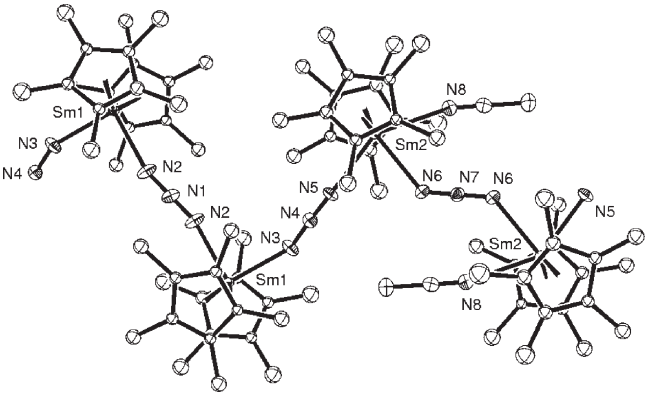

Figure 3. ORTEP of two repeat units of $\{[(C_5Me_5)_2Sm(\mu\text{-}N_3)][(C_5Me_5)_2Sm(NCMe)(\mu\text{-}N_3)]\}_n$, **7**, shown at the 50% probability level. Only one component of the disordered $(C_5Me_5)^-$ ligands is shown. The hydrogen atoms have been omitted for clarity.

The N(azide)−Ln−N(azide) angles for the eight coordinate metals in these complexes are in the range of 88.42(8)−90.89(9)°, but they are smaller for nine coordinate metals, 74.20(7)−76.47(9)°. The absence of an additional coordinating ligand in **4** not only affects these N(azide)−Ln−N(azide) angles but it also allows **4** to adopt the more regular triangular shape than found in **6** and **19**. In the latter molecules, the presence of the extra ligand to one side of the wedge leads to asymmetry in the location of the two azide ligands: one azide is in the center and one is at the side of the wedge. This results in a more kinked structure shown in Figure 2a. A similar arrangement is found in $[(C_5Me_5)_2U(N_3)(\mu\text{-}N_3)]_3$.[51] The N−N bond distances within the azide ligands in **4**, **6**, and **7** are within the conventional range, 1.163(1)−1.182(3) Å, and the N−N−N angles were measured to be between 177.4(3) and 179.997(2)°.

Reactivity of $[(C_5Me_5)_2Ln][(\mu\text{-}Ph)_2BPh_2]$ with Ketones. Slow diffusion of acetone into a solution of **1** in benzene produced pale yellow crystals of $[(C_5Me_5)_2Y(OCMe_2)_2][BPh_4]$, **8**, eq 6. The reaction was repeated in the same manner with **2** and acetone to produce the analogous product $[(C_5Me_5)_2Sm$

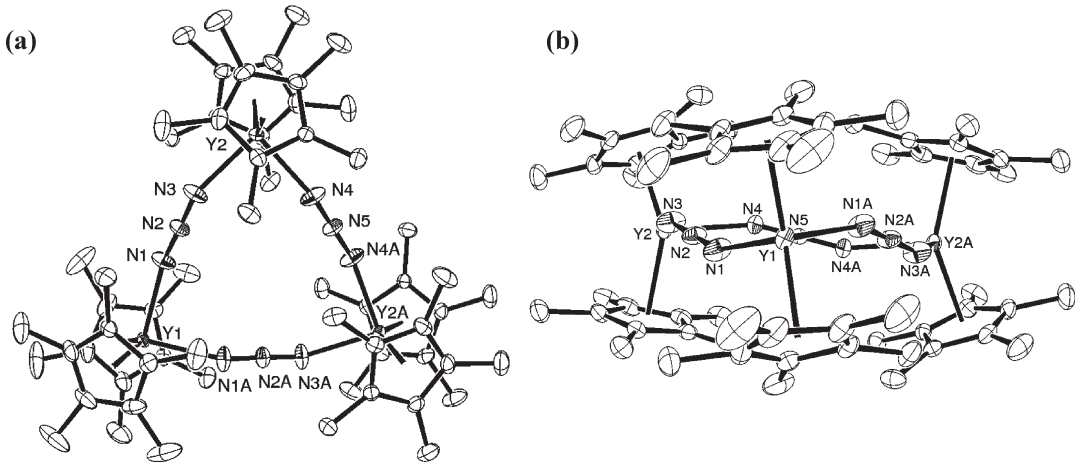

Figure 4. ORTEP of $[(C_5Me_5)_2Y(\mu\text{-}N_3)]_3$, **4**, shown at the 50% probability level from the (a) axial and (b) equatorial viewpoints. The hydrogen atoms have been omitted for clarity.

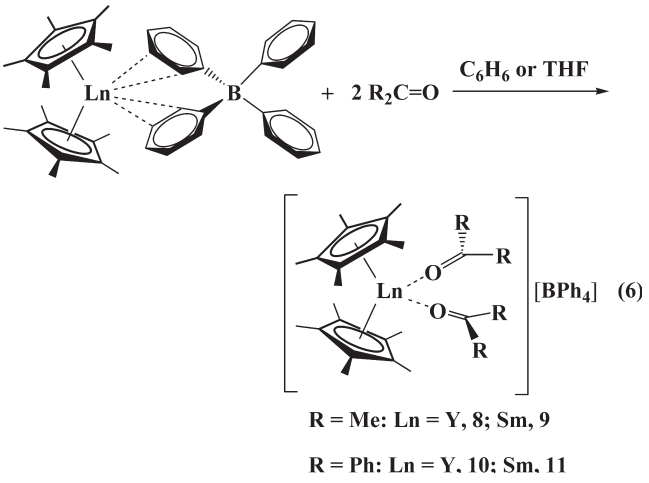

$(OCMe_2)_2][BPh_4]$, **9**, as red-orange crystals. The crystalline products were identified by X-ray crystallography, Figure 5a, and characterized by ^1H and ^{13}C NMR and IR spectroscopy, as well as by mass spectrometry and elemental analysis. Complex **8** was also formed by reacting acetone with the solvated cation, $[(C_5Me_5)_2Y(THF)_2][BPh_4]$, in THF.

Benzophenone reacts with the unsolvated cation complexes **1** and **2** to form the analogous bis(ketone) adducts, $[(C_5Me_5)_2Ln(OCPh_2)_2][BPh_4]$ (Ln = Y, **10**; Sm, **11**), eq 6. Slow evaporation of the filtered reaction solution of **1** and benzophenone deposited red orange crystals of **10**, which were analyzed by X-ray diffraction, Figure 5b. Addition of benzophenone to a THF solution of **1** also yields **10**, as identified by ^1H NMR spectroscopy.

Structural Analysis of $[(C_5Me_5)_2Y(OCMe_2)_2][BPh_4]$, 8, $[(C_5Me_5)_2Sm(OCMe_2)_2][BPh_4]$, 9, and $[(C_5Me_5)_2Y(OCPh_2)_2][BPh_4]$, 10. Table 4 summarizes structural information for **8**−**10**. These formally eight coordinate complexes display metrical parameters typical for lanthanide metallocenes with two additional ligands. Complexes **8** and **9** have very similar structures and the lanthanide based bond distances vary by the difference in ionic radii of eight coordinate Sm^{3+}, 1.079 Å, and Y^{3+}, 1.019 Å.[37] Complex **10** has slightly larger Y−(C_5Me_5 ring centroid) distances and a larger (C_5Me_5 ring centroid)−Y−(C_5Me_5 ring centroid) angle compared to **8**, presumably because of the larger size of the benzophenone ligands versus acetone. The 2.271(1) Å Y−O(acetone) distance in **8** is very similar to the 2.268(1) and 2.261(1) Å Y−O(benzophenone) distances in **10**. Hence, both ketones bind similarly. However, within **10** there are surprising differences. Despite equivalent Y−O(benzophenone) bond lengths, the Y1−O2−C34 and analogous Y1−O1−C21 bond angles are very different: 172.4(1)° and 164.7(1)°. This is another good example of the lack of correlation of bond angle and bond length with oxygen bound ligands.[54,55]

The structure of **9** allows comparisons with $[(C_5Me_5)_2Sm(THF)_2][BPh_4]$, **20**.[11] The two equivalent 2.363(1) Å Sm−O(acetone) distances in **9** are significantly shorter than the 2.46(1) Å Sm−O(THF) distance measured in **20**.[11] However, the 2.423 Å Sm−(C_5Me_5 ring centroid) distance and the 92.9(4)° O−Sm−O and 134.2° (C_5Me_5 ring centroid)−Sm−(C_5Me_5 ring centroid) angles in **20** are very similar to those of **9**. The shorter distances suggest tighter binding of the ketone compared to THF, which is consistent with the THF ligands being displaced by the ketones.

Reactivity of $[(C_5Me_5)_2Ln][(\mu\text{-}Ph)_2BPh_2]$ with Nitrogen Donor Atom Substrates. One equivalent of phenanthroline (phen) reacts with **1** to make yellow $[(C_5Me_5)_2Y(phen)][BPh_4]$, **12**, eq 7, which can be crystallized from THF at −35 °C, Figure 6a. Phenanthroline also reacts with $[(C_5Me_5)_2Y(THF)_2][BPh_4]$ in THF to form **12** as identified by ^1H NMR spectroscopy. Pyridine

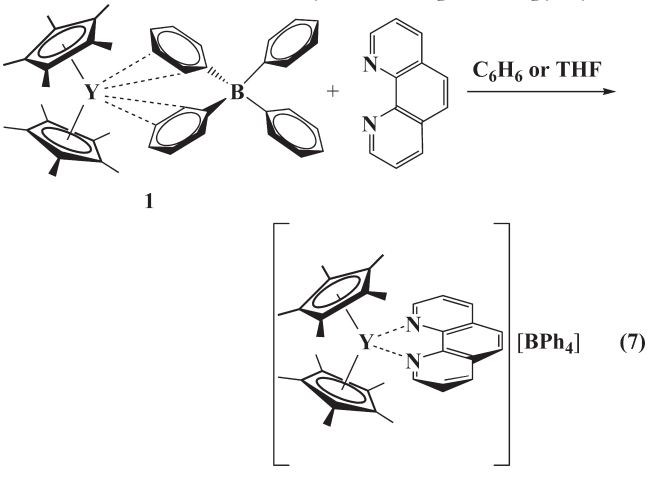

(py) reacts with **1** and **2** to form the bis(pyridine) adducts $[(C_5Me_5)_2Ln(py)_2][BPh_4]$ (Ln = Y, **13**; Sm, **14**), eq 8. Orange

dx.doi.org/10.1021/ic2000409 |*Inorg. Chem.* 2011, 50, 4092–4106

Table 3. Selected Bond Distances (Å) and Angles (deg) for $[(C_5Me_5)_2Y(\mu\text{-}N_3)]_3$, 4, $[(C_5Me_5)_2Sm(NCMe)(\mu\text{-}N_3)]_3$, 6, $\{[(C_5Me_5)_2Sm(\mu\text{-}N_3)][(C_5Me_5)_2Sm(NCMe)(\mu\text{-}N_3)]\}_n$, 7, and $\{(C_5Me_5)_2La[CNN(SiMe_3)_2](\mu\text{-}N_3)\}_3$, 19

	4	6	7	19
Ln−Cnt	2.345, 2.348	2.470, 2.454	2.428, 2.413	2.572, 2.544
		2.460, 2.459	2.443, 2.440	
		2.454, 2.461		
Ln−N(N_3)	2.335(1)	2.435(2)	2.397(2)	2.535(2)
	2.335(1)	2.474(2)	2.400(2)	2.556(3)
	2.321(1), 2.335(1)	2.444(2)	2.473(2)	
		2.474(2)	2.484(2)	
		2.455(2)		
		2.480(2)		
Ln−L[a]		2.588(2)	2.600(2)	2.811(3)
		2.568(2)		
		2.582(2)		
Cnt−Ln−Cnt	139.0, 140.4	138.7, 138.1	137.5, 140.8	139.0
		136.9		
N(N_3)−Ln−N(N_3)	88.42(8)	74.87(7)	90.89(9),	76.47(9)
	88.46(6)	74.20(7)	75.35(8)	
		74.32(7)		

[a] For **6** and **7**, L = N(NCMe); for **19**, L = C[CNN($SiMe_3$)$_2$].

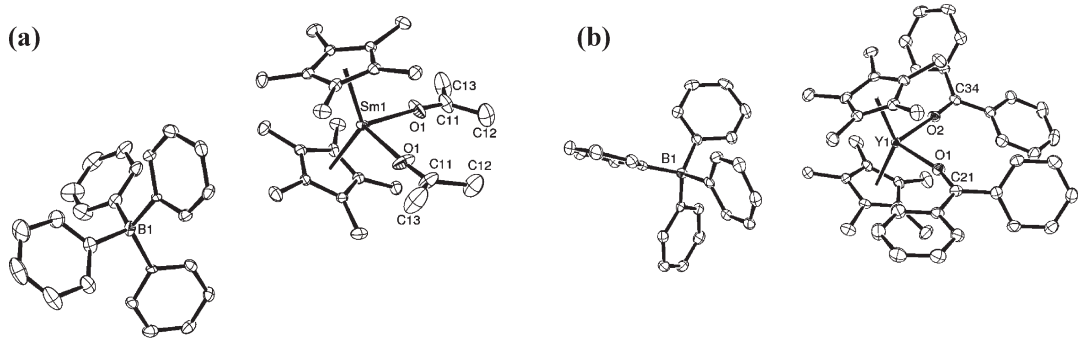

Figure 5. ORTEP of (a) $[(C_5Me_5)_2Sm(OCMe_2)_2][BPh_4]$, **9**, and (b) $[(C_5Me_5)_2Y(OCPh_2)_2][BPh_4]$, **10**, shown at the 50% probability level. Only one component of the disorder in the structure of **9** is shown. The hydrogen atoms have been omitted for clarity. The yttrium acetone analog, **8**, crystallized in a different space group, but has a molecular structure very similar to **9**.

Table 4. Selected Bond Distances (Å) and Angles (deg) for $[(C_5Me_5)_2Y(OCMe_2)_2][BPh_4]$, 8, $[(C_5Me_5)_2Sm(OCMe_2)_2][BPh_4]$, 9, and $[(C_5Me_5)_2Y(OCPh_2)_2][BPh_4]$, 10

$[(C_5Me_5)_2Ln(L)_x][BPh_4]$	8	9	10
Ln−Cnt	2.328	2.391	2.358, 2.366
Ln−O	2.271(1)	2.3633(9), 2.363(1)	2.268(1), 2.261(1)
Cnt−Ln−Cnt	133.6	133.6	140.3
O−Ln−O	91.88(7)	92.55(6)	95.11(5)
Ln−O−C	176.1(1)	174.8(1)	164.7(1), 172.4(1)

crystals of **14** were obtained by diffusion of pyridine into a benzene solution of **2**, Figure 6b. In contrast to the reactions above, **13** and **14** cannot be isolated cleanly from the THF solvated cations.[11] When **13** and **14** are dissolved in THF, $[(C_5Me_5)_2Ln(THF)_2][BPh_4]$ is formed, along with free pyridine.

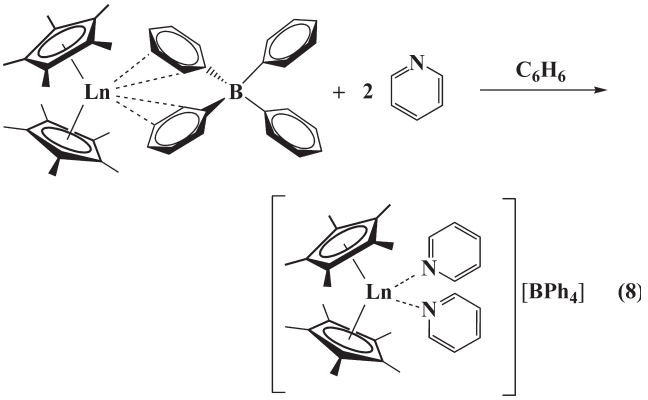

The reaction of **1** with 1 equiv of PhN═NPh in methylcyclohexane yields a brown precipitate over 2 days. The ^{1}H NMR spectrum of this product in C_6D_6 shows a single resonance for

dx.doi.org/10.1021/ic2000409 |Inorg. Chem. 2011, 50, 4092–4106

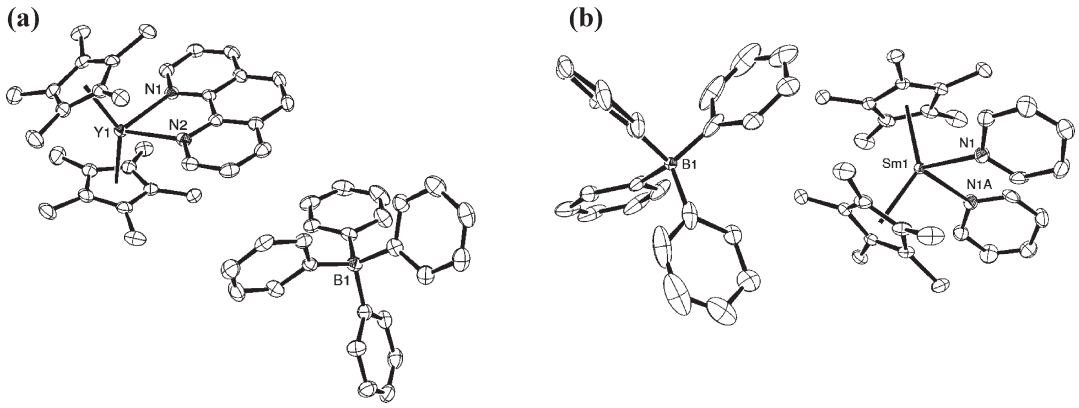

Figure 6. ORTEP of (a) $[(C_5Me_5)_2Y(phen)][BPh_4]$, **12**, and (b) $[(C_5Me_5)_2Sm(py)_2][BPh_4]$, **14**, shown at the 50% probability level. Only one component of the disorder in the structure of **14** is shown. The hydrogen atoms have been omitted for clarity.

two $(C_5Me_5)^-$ groups, a broad aromatic resonance which integrates to 10 protons, and new $(BPh_4)^-$ resonances. A sharp resonance at −5.85 ppm in the ^{11}B NMR spectrum indicates that $(BPh_4)^-$ is present and not BPh_3 (68.0 ppm[47]). The data are consistent with the formation of the azobenzene salt, $[(C_5Me_5)_2Y(PhNNPh)][BPh_4]$, **15**, eq 9. Complex **15** was also characterized by ESI-MS, IR spectroscopy, and elemental analysis.

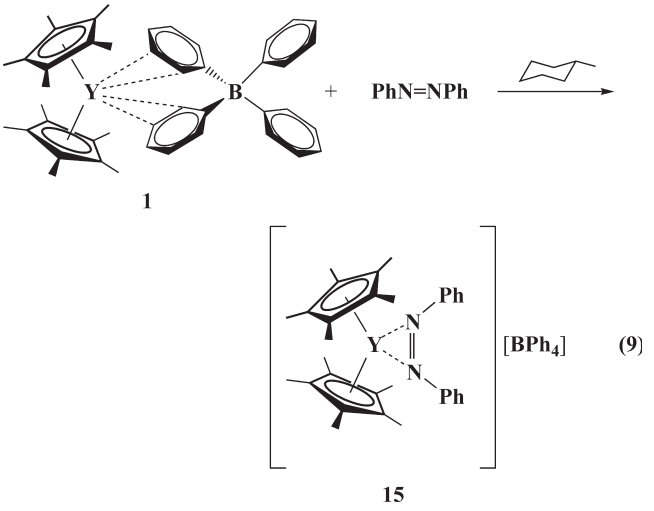

(9)

Complex **15** is sparingly soluble in benzene, and the solution changes color to dark green over 12 h in benzene at room temperature, or upon heating for 2 h in aromatic or aliphatic solvents. The formation of $(C_5Me_5)_2Y(PhNNPh)$, **16**, eq 10, is postulated on the basis of the NMR and EPR spectra of the green crude product mixture. The conversion of **15** to **16** was monitored over the course of 1 day by ^1H and ^{11}B NMR spectroscopy. A decrease in the PhNNPh and $(C_5Me_5)^-$ resonances in the ^1H NMR spectrum of **15** was observed, along with the conversion of $(BPh_4)^-$ to BPh_3 in the ^{11}B NMR spectrum. Complex **16** can be separated from residual, less soluble **15** by alkane extraction, but the BPh_3 and Ph_2 byproducts are difficult to separate from **16** because of their similar solubilities. BPh_3 could be separated by sublimation of the mixture at 100 °C under high vacuum (10^{-5} Torr), but azobenzene also sublimed, which suggested that **16** is not stable under these conditions.

The EPR spectrum of **16**, Figure 7a, shows five major resonances separated by 8.25 G, which is the splitting pattern expected for an unpaired electron coupled to two ^{14}N nuclei (I = 1). Typical ^{14}N hyperfine coupling constants for free $(PhNNPh)^-$ are around 4 to 5 G.[56,57] The EPR spectrum also shows hyperfine splitting attributable to coupling of an unpaired electron with the protons on the phenyl rings of $(PhNNPh)^-$. The ^1H coupling constants were determined through simulation to be 0.95 and 2.40 G. Proton hyperfine coupling constants of K(PhNNPh) are found to be in the range of 0.61 to 3.20 G.[57,58] Coupling to a single ^{89}Y nucleus is also observed, with a coupling constant of 1.95 G. The simulated EPR spectrum with these parameters, Figure 7b, agrees well with the experimental data. An isotropic g value of 2.004 was measured for **16** using DPPH as a calibrant. This suggests that the radical is mainly ligand-centered. The NMR and EPR data are consistent with a $(PhNNPh)^-$ radical and the formation of $(C_5Me_5)_2Y(PhNNPh)$ according to eq 10.

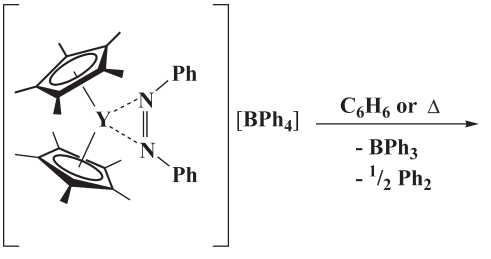

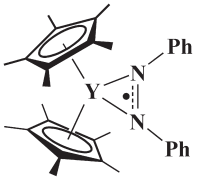

(10)

The reaction of **1** with phenazine in benzene is similar to the azobenzene reaction above, in that a radical product $\{[(C_5Me_5)_2Y]_2(phz)\}\{BPh_4\}$, **17**, is formed, eq 11. Complex **17** is NMR silent, and its EPR spectrum strongly supports the presence of the radical monoanion $(phz)^-$. The EPR spectrum, Figure 7c, also shows five major resonances attributable to

dx.doi.org/10.1021/ic2000409 |*Inorg. Chem.* 2011, 50, 4092–4106

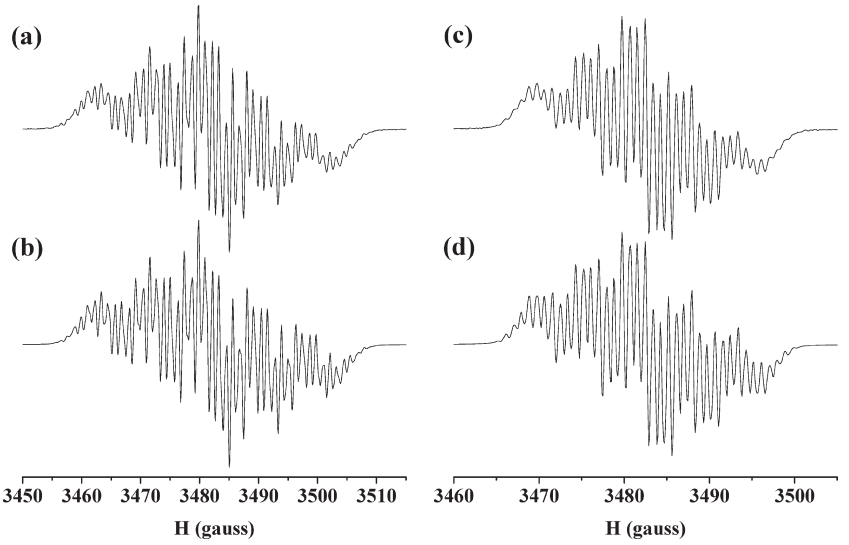

Figure 7. EPR spectra of (a) $(C_5Me_5)_2Y(PhNNPh)$, **16**, in hexane at room temperature, (b) simulation of **16**, (c) $\{[(C_5Me_5)_2Y]_2(phz)\}\{BPh_4\}$, **17**, in benzene at room temperature, and (d) simulation of **17**.

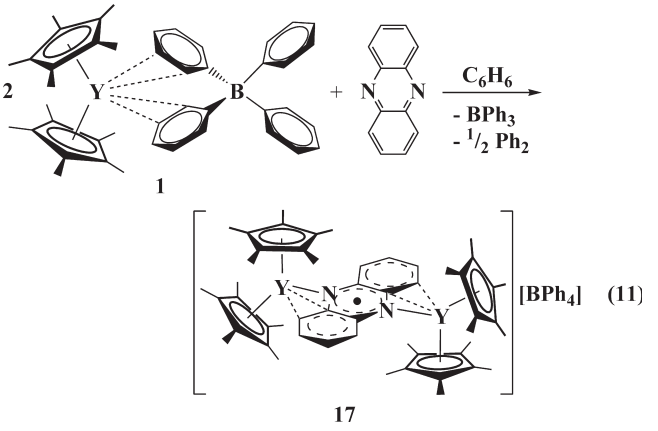

coupling with two ^{14}N nuclei in phenazine. A ^{14}N coupling constant of 5.44 G was determined by simulation, which is in the 3.6 to 6.8 G range for ^{14}N coupling constants of known phenazine radical anions.[59,60] The hyperfine splitting in the spectrum shows a pattern consistent with an unpaired electron coupled to eight protons and two yttrium nuclei. The ^1H coupling constants were determined via spectral simulation to be 1.68 and 0.95 G, which are in the 0.72 to 2.53 G range for proton coupling constants of coordinated phenazine radical anions.[59] A coupling constant of 1.18 G for both ^{89}Y nuclei was also determined in the simulation process. The simulated EPR spectrum, Figure 7d, agrees well with the experimental data. The *g* value for this spectrum was measured to be 2.005, consistent with a ligand-centered radical. No reaction occurs between the solvate, $[(C_5Me_5)_2Y(THF)_2][BPh_4]$, and phenazine.

Slow diffusion of hexane into a concentrated green solution of **17** in benzene yielded dark green X-ray quality crystals, Figure 8a. Red crystals of the phenazine dianion complex $[(C_5Me_5)_2Y]_2(phz)$, **18**, formed from an NMR sample of **17** in benzene-d_6 over several weeks at room temperature. Complex **18** was characterized by X-ray crystallography, Figure 8b.

Complex **18** can also be formed by heating **17** at 70 °C in C_6D_6 over 2 days. The ^1H NMR spectrum of the resulting red solution showed **18** to be the major product along with resonances for BPh_3 and Ph_2. Resonances for 5,10-dihydrophenazine, $phzH_2$, were also identified by independent synthesis[49] and determination of its ^1H NMR spectrum in C_6D_6. The slow conversion of **17** to **18** can be described by a second one-electron reduction of the phenazine radical anion in **17** by $(BPh_4)^-$, eq 12.

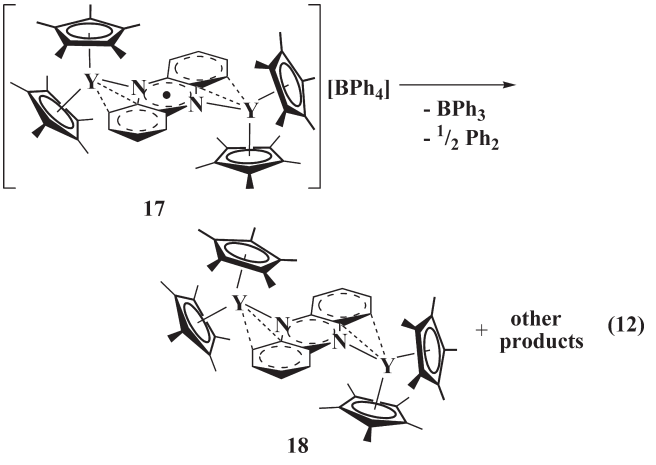

Table 5. Selected Bond Distances (Å) and Angles (deg) for $[(C_5Me_5)_2Y(phen)][BPh_4]$, 12, $[(C_5Me_5)_2Sm(py)_2][BPh_4]$, 14, and $[(C_5Me_5)_2Yb(phen)][I]$, 21

$[(C_5Me_5)_2Ln(L)_x][BPh_4]$	12	14	21
Ln−Cnt	2.343, 2.354	2.417	
Ln−N	2.403(2), 2.413(2)	2.540(1)	2.339(8), 2.382(8)
Cnt−Ln−Cnt	144.2	137.2	
N−Ln−N	69.46(7)	90.98(6)	70.3(3)

Structural Analysis of Nitrogen-Donor Complexes. Table 5 shows the metrical data for $[(C_5Me_5)_2Y(phen)][BPh_4]$, **12**, and $[(C_5Me_5)_2Sm(py)_2][BPh_4]$, **14**, along with comparison data for

dx.doi.org/10.1021/ic2000409 |*Inorg. Chem.* 2011, 50, 4092–4106

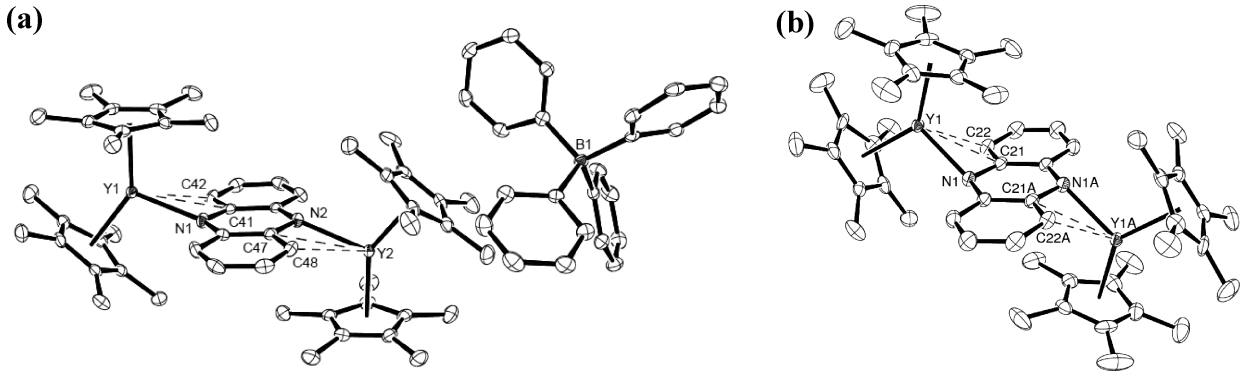

Figure 8. ORTEP of (a) $\{[(C_5Me_5)_2Y]_2(phz)\}\{BPh_4\}$, **17**, and (b) $[(C_5Me_5)_2Y]_2(phz)$, **18**, shown at the 50% probability level. The hydrogen atoms have been omitted for clarity.

Table 6. Selected Bond Distances (Å), Angles (deg), and Metal Displacements out of the Phenazine Plane for $\{[(C_5Me_5)_2Y]_2(phz)\}\{BPh_4\}$, 17, $[(C_5Me_5)_2Y]_2(phz)$, 18, $[(C_5Me_5)_2Sm]_2(phz)$, 22, and $[(C_5Me_4H)_2Lu]_2(phz)$, 23

	17	18	22	23
Ln−Cnt	2.318, 2.325	2.366, 2.346	2.421, 2.436	2.301, 2.272
	2.320, 2.326			2.275, 2.299
Ln−N	2.358(2)	2.298(1)	2.360(2)	2. 248(2)
	2.3545(19)			2.231(2)
Ln−C_α[a]	3.062(2) 3.060(2)	2.817(2)	2.877(2)	2.755(3)
				2.762(3)
Ln−C_β[b]	3.028(2) 3.028(2)	2.785(2)	2.866(3)	2.719(3)
				2.762(3)
Cnt−Ln−Cnt	142.8, 142.4	137.0	136.4	133.5, 133.7
Ln−N−(phz plane)[c]	160.9, 158.9	144.5	140.4	148.6, 149.9
Ln displacement	0.8486, 0.8150	1.3523	1.5249	1.2223, 1.0990

[a] C_α = C41, C47 for **17**; C21 for **18**. [b] C_β = C42, C48 for **17**; C22 for **18**. [c] Plane defined by the 6 atoms in the central ring of phenazine.

$[(C_5Me_5)_2Yb(phen)][I]$, **21**.[31] The structures of **12** and **21** have similar metal−ligand bond distances within the error limits when the difference in the eight coordinate ionic radii is considered: 1.019 Å for Y^{3+} versus 0.985 Å for Yb^{3+}.[37] The bond distances in the neutral phenanthroline ligands are also quite similar. However, the plane of the phenanthroline ligand in **12** is tilted only 1° from the plane that bisects the metallocene wedge, whereas the analogous angle is 15° in **21**.

The symmetry equivalent neutral pyridine molecules coordinated to samarium in complex **14** have a 2.540(1)Å Sm−N distance that is similar to the 2.576(3) Å value in $[(C_5Me_2)Sm(py)]_2(\mu\text{-}O)$.[61] The Sm−N distances in **14** are, on average, 0.132 Å longer than the Y−N distances in **12**, which is 0.072 Å more than expected when only the differences in ionic radii are considered. It may be the chelating ability of phenanthroline that allows it to bind more tightly than two separate pyridine ligands.

Crystallographic data on the structures of $\{[(C_5Me_5)_2Y]_2(phz)\}\{BPh_4\}$, **17**, and $[(C_5Me_5)_2Y]_2(phz)$, **18**, are presented in Table 6, along with that of $[(C_5Me_5)_2Sm]_2(phz)$,[14] **22**, and $[(C_5Me_4H)_2Lu]_2(phz)$,[18] **23**. The structures of **17** and **18** allow the first comparison of a phenazine monoanion and a phenazine dianion in rare earth metallocenes. Significant differences exist between **17** and the other structures. The 2.354(2) and 2.358(2) Å Y−N distances in **17** are longer than the 2.298(1) Å Y−N distance in **18**, and the Y···C(phz) distances are over 0.2 Å longer in **17**. Hence, as expected, the phenazine dianion in **18** interacts more strongly with yttrium than does the monoanion in **17**. In addition, the metal atoms in **17** approach the phenazine plane at a more obtuse angle, that is, the Ln−N−(phz plane) angles are 158.9−160.9° in **17** versus 140.4−149.9° in the $(phz)^{2-}$ examples in Table 6. This is consistent with the fact that as phenazine is successively reduced by one and then two electrons, aromaticity decreases and the hybridization of the nitrogen atoms is shifted from sp^2 toward sp^3.

Fluorenone. The combination of **1** and fluorenone produces a dark burgundy precipitate in benzene within 20 min. The ^1H NMR spectrum of the isolated product in THF-d_8 is consistent with a mono(fluorenone) adduct salt, $[(C_5Me_5)_2Y(OC_7H_8)(THF)_x][BPh_4]$. The same NMR sample gave an EPR spectrum that is consistent with a fluorenone radical, Figure 9a. A simulated EPR spectrum, Figure 9b, agrees well with the experimental data, displaying ^1H coupling constants due to 8 protons, 3.36 G (2H), 0.73 G (2H), 2.76 G (2H), 0.61 G (2H), and an ^{89}Y coupling constant due to one yttrium nucleus, 0.63 G. The measured g value is 2.003, which is characteristic of a ligand-based radical. BPh_3 was identified in the dark burgundy THF solution by ^{11}B NMR spectroscopy, suggesting the same type of $(BPh_4)^-$ reduction observed with azobenzene and phenazine may be occurring with fluorenone to form a complex such as "$(C_5Me_5)_2Y(OC_7H_8)$." However, attempts to isolate such a complex in pure crystalline form were unsuccessful.

dx.doi.org/10.1021/ic2000409 |*Inorg. Chem.* 2011, 50, 4092–4106

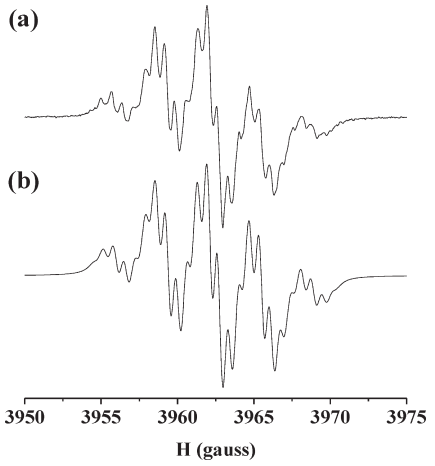

Figure 9. (a) EPR spectrum of a millimolar solution of "$[(C_5Me_5)_2Y(OC_7H_8)(THF)_x][BPh_4]$" in THF at room temperature. (b) Simulated spectrum.

DISCUSSION

$[(C_5Me_5)_2Y][(\mu\text{-Ph})_2BPh_2]$, **1**, and $[(C_5Me_5)_2Sm][(\mu\text{-Ph})_2BPh_2]$, **2**, readily react with NaN_3 to provide the $[(C_5Me_5)_2Ln(N_3)]_x$ compounds that were desired as models for the postulated $[(C_5Me_5)_2UN_3]_x$ intermediate in the formation of $[(C_5Me_5)_2U(\mu\text{-N})U(\mu\text{-N}_3)(C_5Me_5)_2]_4$ from NaN_3 and $[(C_5Me_5)_2U][(\mu\text{-Ph})_2BPh_2]$.[19] The unsolvated azide complexes are not very soluble, as is typical with $[(C_5Me_5)_2Ln(\text{bridging ligand})]_x$ complexes where the bridging ligand is a halide[4,62] or a pseudohalide[63−68] like cyanide. This is generally attributed to extended bridging structures. Complexes of this type are often crystallographically characterizable as Lewis base (L) adducts, and they are usually obtained as trimers, that is, $[(C_5Me_5)_2Ln(L)(\text{bridging ligand})]_3$. This is the case with the samarium azide, $[(C_5Me_5)_2Sm(\mu\text{-}N_3)]_x$, **5**, that could be crystallographically characterized as the acetonitrile adduct, $[(C_5Me_5)_2Sm(NCMe)(\mu\text{-}N_3)]_3$, **6**. Interestingly, complex **5** could also be crystallized in a different solvated form, one in which there is only one coordinating ligand per two metals, $\{[(C_5Me_5)_2Sm(\mu\text{-}N_3)][(C_5Me_5)_2Sm(NCMe)(\mu\text{-}N_3)]\}_n$, **7**. In the absence of 1:1 Lewis base to metal ligation, an extended polymer is formed in **7** via Sm−NNN−Sm bridges.

In the yttrium case, crystals of an unsolvated complex, $[(C_5Me_5)_2Y(\mu\text{-}N_3)]_3$, **4**, were fortuitously obtained when this complex was synthesized via a reduction reaction involving 1-adamantyl azide and **1**. This was the first example in this study whereby a tetraphenylborate ligand acts as a non-innocent counter-anion: it can act as a reductant as shown in eq 3. Additional examples are discussed below.

Formation of the azide complexes **3** and **5** did not require the unsolvated cations, **1** and **2**, since these reactions could also be conducted in THF. The fact that an inorganic azide reacts with $[(C_5Me_5)_2Ln(THF)_2][BPh_4]$ (Ln = Y, Sm) to form unsolvated $[(C_5Me_5)_2Ln(N_3)]_x$ species contrasts sharply with the reaction of $(C_5Me_5)^-$ with the solvated cations that leads to nucleophilic ring-opening of the bound THF to make $(C_5Me_5)_2Ln[O(CH_2)_4C_5Me_5](THF)$.[69]

The reactions of the lanthanide metallocene cations with ketones are also unaffected by the absence or presence of THF. Hence the acetone adducts, $[(C_5Me_5)_2Ln(OCMe_2)_2][BPh_4]$, **8** and **9**, and the benzophenone complexes $[(C_5Me_5)_2Ln(OCPh_2)_2][BPh_4]$, **10** and **11**, can be generated from both $[(C_5Me_5)_2Ln][(\mu\text{-Ph})_2BPh_2]$ and $[(C_5Me_5)_2Ln(THF)_2][BPh_4]$, eq 6. However, the reactions with phenanthroline and pyridine differ in terms of their sensitivity to the presence of THF. $[(C_5Me_5)_2Y(phen)][BPh_4]$, **12**, can be made from **1** or its THF adduct, but addition of THF to the pyridine complexes, $[(C_5Me_5)_2Ln(py)_2][BPh_4]$, **13** and **14**, forms the THF adducts, $[(C_5Me_5)_2Ln(THF)_2][BPh_4]$. The chelating effect of phenanthroline could explain why it is not displaced by THF in **12** as pyridine is in **13** and **14**.

Reductive reactivity facilitated by the tetraphenylborate ion via eq 3 was also observed in the reaction of **1** with azobenzene. Lanthanide based reductions of azobenzene have been extensively studied.[17,20−24] Although evidence for the azobenzene adduct, $[(C_5Me_5)_2Y(PhNNPh)][BPh_4]$, **15**, was obtained, this product is not stable with respect to the neutral complex free of $(BPh_4)^-$, namely, $(C_5Me_5)_2Y(PhNNPh)$, **16**. An analogous complex of samarium had previously been obtained through reduction of PhN=NPh by the divalent complex, $(C_5Me_5)_2Sm(THF)_2$, and fully characterized by X-ray crystallography as the THF adduct, $(C_5Me_5)_2Sm(PhNNPh)(THF)$.[20] However, this species could not be fully characterized by EPR spectroscopy because of the paramagnetic $4f^5$ Sm^{3+} ion. In contrast, the EPR spectrum of **16** clearly indicated the presence of the $(PhNNPh)^-$ radical anion.

Since phenazine (−0.36 V vs SCE)[70] and fluorenone (−1.30 V vs SCE)[71] are more easily reduced than azobenzene (−1.35 to −1.41 V vs SCE),[72] it was not surprising that they too are reduced by **1** via eq 3. The EPR spectra of these products suggested formation of the radical monoanions $(phz)^-$ and $(OC_7H_8)^-$, respectively. In the phenazine case, the structure was confirmed by X-ray crystallography as $\{[(C_5Me_5)_2Y]_2(phz)\}\{BPh_4\}$, **17**.

Hence, the reductive reactivity of the tetraphenylborate anion in $[(C_5Me_5)_2Y][(\mu\text{-Ph})_2BPh_2]$ has some generality. Although the long known $(BPh_4)^-$ reductive reactivity[38−46] had recently been observed in f element complexes, it was generally in combination with a redox active metal such as uranium or samarium. In **1**, the $(BPh_4)^-$ effects reduction without any concomitant metal redox reaction.

CONCLUSION

The unsolvated cations, $[(C_5Me_5)_2Y][(\mu\text{-Ph})_2BPh_2]$, **1**, and $[(C_5Me_5)_2Sm][(\mu\text{-Ph})_2BPh_2]$, **2**, have provided a useful approach to examine the initial coordination of Lewis basic substrates to lanthanide metallocenes. They react readily with a variety of substrates by displacement of the weakly coordinated $(BPh_4)^-$ anion. Although this type of reactivity was expected, it was not anticipated that $(BPh_4)^-$ would also show reductive reactivity in these complexes. The one electron redox chemistry of this anion in the presence of the metallocene cation has provided complexes of radical anions that were previously unavailable from reductions with Ln^{2+} reagents like $(C_5Me_5)_2Ln(THF)_x$, Ln = Eu, Yb, and Sm. The isolation of the first rare earth $(phenazine)^-$ complex, $\{[(C_5Me_5)_2Y]_2(phz)\}\{BPh_4\}$, shows the power of combining the reductive reactivity of the $(BPh_4)^-$ anion with the coordinating and stabilizing capacity of rare earth metallocene cations.

ASSOCIATED CONTENT

Supporting Information. X-ray data collection, structure solution, and refinement (PDF) and X-ray diffraction details of compounds **4**, **6**, **7**, **8**, **9**, **10**, **12**, **14**, **17**, **18** (CIF, CCDC No.

803836−803845). This material is available free of charge via the Internet at http://pubs.acs.org.

AUTHOR INFORMATION

Corresponding Author
*Fax: 949-824-2210. E-mail: wevans@uci.edu.

ACKNOWLEDGMENT

We thank the U.S. National Science Foundation for support of this research and Dr. Michael K. Takase and Ryan A. Zarkesh for assistance with X-ray crystallography.

REFERENCES

(1) Evans, W. J.; Seibel, C. A.; Ziller, J. W. *J. Am. Chem. Soc.* **1998**, *120*, 6745–6752.
(2) Evans, W. J.; Davis, B. L.; Champagne, T. M.; Ziller, J. W. *Proc. Natl. Acad. Sci. U.S.A.* **2006**, *103*, 12678–12683.
(3) Evans, W. J.; Nyce, G. W.; Forrestal, K. J.; Ziller, J. W. *Organometallics* **2002**, *21*, 1050–1055.
(4) Evans, W. J.; Perotti, J. M.; Kozimor, S. A.; Champagne, T. M.; Davis, B. L.; Nyce, G. W.; Fujimoto, C. H.; Clark, R. D.; Johnston, M. A.; Ziller, J. W. *Organometallics* **2005**, *24*, 3916–3931.
(5) Evans, W. J.; Perotti, J. M.; Ziller, J. W. *J. Am. Chem. Soc.* **2005**, *127*, 3894–3909.
(6) Evans, W. J.; Perotti, J. M.; Ziller, J. W. *J. Am. Chem. Soc.* **2005**, *127*, 1068–1069.
(7) Evans, W. J.; Perotti, J. M.; Ziller, J. W. *J. Am. Chem. Soc.* **2006**, *128*, 16178–16189.
(8) Evans, W. J.; Kozimor, S. A.; Ziller, J. W. *Chem. Commun.* **2005**, *37*, 4681–4683.
(9) Dietrich, H. M.; Ziller, J. W.; Anwander, R.; Evans, W. J. *Organometallics* **2009**, *28*, 1173–1179.
(10) Evans, W. J. *Inorg. Chem.* **2007**, *46*, 3435–3449.
(11) Evans, W. J.; Ulibarri, T. A.; Chamberlain, L. R.; Ziller, J. W.; Alvarez, D. A., Jr. *Organometallics* **1990**, *9*, 2124–2130.
(12) Schumann, H.; Glanz, M.; Hemling, H.; Görlitz, F. H. *J. Organomet. Chem.* **1993**, *462*, 155–161.
(13) Evans, W. J.; Gonzales, S. L.; Ziller, J. W. *J. Am. Chem. Soc.* **1991**, *113*, 7423–7424.
(14) Evans, W. J.; Gonzales, S. L.; Ziller, J. W. *J. Am. Chem. Soc.* **1994**, *116*, 2600–2608.
(15) Evans, W. J.; Davis, B. L. *Chem. Rev.* **2002**, *102*, 2119–2136.
(16) Evans, W. J.; Miller, K. A.; Lee, D. S.; Ziller, J. W. *Inorg. Chem.* **2005**, *44*, 4326–4332.
(17) Evans, W. J.; Lee, D. S.; Ziller, J. W.; Kaltsoyannis, N. *J. Am. Chem. Soc.* **2006**, *128*, 14176–14184.
(18) Evans, W. J.; Lorenz, S. E.; Ziller, J. W. *Inorg. Chem.* **2009**, *48*, 2001–2009.
(19) Evans, W. J.; Kozimor, S. A.; Ziller, J. W. *Science* **2005**, *309*, 1835–1838.
(20) Evans, W. J.; Drummond, D. K.; Chamberlain, L. R.; Doedens, R. J.; Bott, S. G.; Zhang, H.; Atwood, J. L. *J. Am. Chem. Soc.* **1988**, *110*, 4983–4994.
(21) Evans, W. J.; Champagne, T. M.; Ziller, J. W. *Organometallics* **2007**, *26*, 1204–1211.
(22) Trifonov, A. A.; Bochkarev, M. N.; Schumann, H.; Loebel, J. *Angew. Chem., Int. Ed. Engl.* **1991**, *30*, 1149–1151.
(23) Turcitu, D.; Nief, F.; Ricard, L. *Chem.—Eur. J.* **2003**, *9*, 4916–4923.
(24) Pan, C.-L.; Chen, W.; Song, S.; Zhang, H.; Li, X. *Inorg. Chem.* **2009**, *48*, 6344–6346.
(25) Evans, W. J.; Walensky, J. R.; Champagne, T. M.; Ziller, J. W.; DiPasquale, A. G.; Rheingold, A. L. *J. Organomet. Chem.* **2009**, *694*, 1238–1243.
(26) Scholz, J.; Scholz, A.; Weimann, R.; Janiak, C.; Schumann, H. *Angew. Chem., Int. Ed.* **1994**, *33*, 1171–1174.
(27) Evans, W. J.; Takase, M. K.; Ziller, J. W.; DiPasquale, A. G.; Rheingold, A. L. *Organometallics* **2009**, *28*, 236–243.
(28) Evans, W. J.; Schmiege, B. M.; Lorenz, S. E.; Miller, K. A.; Champagne, T. M.; Ziller, J. W.; DiPasquale, A. G.; Rheingold, A. L. *J. Am. Chem. Soc.* **2008**, *130*, 8555–8563.
(29) Hou, Z.; Wakatsuki, Y. *Chem.—Eur. J.* **1997**, *3*, 1005–1008.
(30) Hou, Z.; Fujita, A.; Zhang, Y.; Miyano, T.; Yamazaki, H.; Wakatsuki, Y. *J. Am. Chem. Soc.* **1998**, *120*, 754–766.
(31) Schultz, M.; Boncella, J. M.; Berg, D. J.; Tilley, T. D.; Anderson, R. A. *Organometallics* **2002**, *21*, 460–472.
(32) Fedushkin, I. L.; Nevodchikov, V. I.; Bochkarev, M. N.; Dechert, S.; Schumann, H. *Russ. Chem. Bull., Int. Ed.* **2003**, *52*, 154–159.
(33) Hou, Z.; Miyano, T.; Yamazaki, H.; Wakatsuki, Y. *J. Am. Chem. Soc.* **1995**, *117*, 4421–4422.
(34) Hou, Z.; Fujita, A.; Yamazaki, H.; Wakatsuki, Y. *J. Am. Chem. Soc.* **1996**, *118*, 7843–7844.
(35) Evans, W. J.; Montalvo, E.; Champagne, T. M.; Ziller, J. W.; DiPasquale, A. G.; Rheingold, A. L. *J. Am. Chem. Soc.* **2008**, *130*, 16–17.
(36) Schumann, H.; Janiak, C.; Pickardt *J. Organomet. Chem.* **1988**, *349*, 117–122.
(37) Shannon, R. D. *Acta Crystallogr.* **1976**, *A 32*, 751–767.
(38) Wittig, V. G.; Raff, P. *Justus Liebigs Ann. Chem.* **1951**, *573*, 195–209.
(39) Williams, J. L. R.; Doty, J. C.; Grisdale, P. J.; Searle, R.; Regan, T. H.; Happ, G. P.; Maier, D. P. *J. Am. Chem. Soc.* **1967**, *89*, 5153–5157.
(40) Grisdale, P. J.; Williams, J. L. R.; Glogowski, M. E.; Babb, B. E. *J. Org. Chem.* **1971**, *36*, 544–549.
(41) Eisch, J. J.; Boleslawski, M. P.; Tamao, K. *J. Org. Chem.* **1989**, *54*, 1627–1634.
(42) Wilkey, J. D.; Schuster, G. B. *J. Am. Chem. Soc.* **1991**, *113*, 2149–2155.
(43) Strauss, S. H. *Chem. Rev.* **1993**, *93*, 927–942.
(44) Eisch, J. J.; Shah, J. H.; Boleslawski, M. P. *J. Organomet. Chem.* **1994**, *464*, 11–21.
(45) Crawford, C. L.; Barnes, M. J.; Peterson, R. A.; Wilmarth, W. R.; Hyder, M. L. *J. Organomet. Chem.* **1999**, *581*, 194–206.
(46) Pal, P. K.; Chowdhury, S.; Drew, M. G. B.; Datta, D. *New. J. Chem.* **2002**, *26*, 367–371.
(47) Nöth, H.; Wrackmeyer, B. In *NMR, Basic Principles and Progress*; Diehl, P., Fluck, E., Kosfeld, R., Eds.; Springer-Verlag: Berlin, 1978; Vol. 14.
(48) Duling, D. R. *PEST WinSIM*; NIEHS: Research Triangle Park, NC, 1996.
(49) Sugimoto, A.; Kotani, T.; Tsujimoto, J.; Yoneda, S. *J. Heterocycl. Chem.* **1989**, *26*, 435–438.
(50) Dori, Z.; Ziolo, R. F. *Chem. Rev.* **1973**, *73*, 247–254.
(51) Evans, W. J.; Miller, K. A.; Ziller, J. W.; J., G. *Inorg. Chem.* **2007**, *46*, 8008–8018.
(52) Farrugia, L. J. *J. Appl. Crystallogr.* **1997**, *30*, 565.
(53) Evans, W. J.; Foster, S. E. *J. Organomet. Chem.* **1992**, *433*, 79–94.
(54) Steffey, B. D.; Fanwick, P. E.; Rothwell, I. P. *Polyhedron* **1990**, *9*, 963–968.
(55) Howard, W. A.; Trnka, T. M.; Parkin, G. *Inorg. Chem.* **1995**, *34*, 5900–5909.
(56) Russell, G. A.; Konaka, R.; Strom, E. T.; Danen, W. C.; Chang, K.; Kaupp, G. *J. Am. Chem. Soc.* **1968**, *90*, 4646–4653.
(57) Johnson, C. S., Jr.; Chang, R. *J. Chem. Phys.* **1965**, *43*, 3183–3192.
(58) Buser, U.; Ess, C. H.; Gerson, F. *Magn. Reson. Chem.* **1991**, *29*, 721–725.

(59) Jacobsen, G. E.; Raston, C. L. *J. Organomet. Chem.* **1990**, *395*, C1–C4.
(60) Eloranta, J.; Salo, E.; Mäkinen, S. *Acta Chem. Scand. A* **1980**, *34*, 427–432.
(61) Evans, W. J.; Davis, B. L.; Nyce, G. W.; Perotti, J. M.; Ziller, J. W. *J. Organomet. Chem.* **2003**, *677*, 89–95.
(62) Evans, W. J.; Drummond, D. K.; Grate, J. W.; Zhang, H.; Atwood, J. L. *J. Am. Chem. Soc.* **1987**, *109*, 3928–3936.
(63) Radu, N. S.; Hollander, F. J.; Tilley, T. D.; Rheingold, A. L. *Chem. Commun.* **1996**, 2459–2460.
(64) Evans, W. J.; Forrestal, K. J.; Ziller, J. W. *J. Am. Chem. Soc.* **1998**, *120*, 9273–9282.
(65) Evans, W. J.; Drummond, D. K. *Organometallics* **1988**, *7*, 797–802.
(66) Maynadié, J.; Berthet, J.-C.; Thuéry, P.; Ephritikhine, M. *Organometallics* **2007**, *26*, 2623–2629.
(67) Evans, W. J.; Montalvo, E.; Foster, S. E.; Harada, K. A.; Ziller, J. W. *Organometallics* **2007**, *26*, 2904–2910.
(68) Evans, W. J.; Montalvo, E.; Champagne, T. M.; Ziller, J. W.; DiPasquale, A. G.; Rheingold, A. L. *Organometallics* **2009**, *28*, 2897–2903.
(69) Evans, W. J.; Forrestal, K. J.; Leman, J. T.; Ziller, J. W. *Organometallics* **1996**, *15*, 527–531.
(70) de Boer, E. *Adv. Organomet. Chem.* **1964**, *2*, 115–155.
(71) Behrendt, A.; Screttas, C. G.; Bethell, D.; Schiemann, O.; Stelle, B. R. *J. Chem. Soc., Perkin Trans. 2* **1998**, 2039–2045.
(72) Thomas, F. G.; Boto, K. G. *The Chemistry of the Hydrazo, Azo, and Azoxy Groups*; Patai, S., Ed.; Wiley: New York, 1975; Chapter 12.